

Mononuclear NHC–Pd– π -Allyl Complexes Containing Weakly Coordinating Ligands

Eleonora S. Chernyshova, Richard Goddard, and Klaus-Richard Pörschke*

Max-Planck-Institut für Kohlenforschung, D-45466 Mülheim an der Ruhr, Germany

Received March 9, 2007

Attempts are described to synthesize ionic $14e$ $[(\pi\text{-allyl})\text{Pd}(\text{NHC})]\text{Y}$ complexes (NHC = $\text{C}(\text{N}(\text{tBu})\text{CH}_2)$, $\text{C}(\text{N}(\text{C}_6\text{H}_3\text{-}2,6\text{-iPr}_2)\text{CH}_2)$). Reaction of $\{(\eta^3\text{-}2\text{-RC}_3\text{H}_4)\text{Pd}(\mu\text{-Cl})\}_2$ (R = H, Me) with AgOTf yields polymeric, helical $\{(\eta^3\text{-C}_3\text{H}_5)\text{Pd}(\mu\text{-OTf})\}_n$ (**5a**) and dimeric $\{(\eta^3\text{-}2\text{-MeC}_3\text{H}_4)\text{Pd}(\mu\text{-OTf})\}_2$ (**5b**). Treatment of $(\eta^3\text{-}2\text{-RC}_3\text{H}_4)\text{Pd}(\text{NHC})\text{Cl}$ (R = H, Me) (**6a–d**) with LiMe or $(\text{tmeda})\text{MgMe}_2$ affords the Pd–methyl complexes $(\eta^3\text{-}2\text{-RC}_3\text{H}_4)\text{Pd}(\text{NHC})\text{CH}_3$ (**7a–d**). Adduct formation of **5a,b** with NHC, metathesis of **6a–d** with AgOTf , and protolysis of **7c,d** with HOTf yield the triflate complexes $(\eta^3\text{-}2\text{-RC}_3\text{H}_4)\text{Pd}(\text{NHC})(\text{OTf})$ (**8a–d**), whereas protolysis of **7a,b** with acids (HOTf , HBF_4) results in complex degradation. From the reactions of **6a,c** with AgBF_4 in THF, and AgPF_6 and $\text{AgAIR}^{\text{F}_4}$ (R^F = $\text{OC}(\text{CF}_3)_3$) in THF and CH_2Cl_2 , respectively, the ionic THF-solvates $[(\eta^3\text{-C}_3\text{H}_5)\text{Pd}\{\text{C}(\text{N}(\text{tBu})\text{CH}_2)\}(\text{THF})]\text{Y}$ (Y = BF_4 , **9a**(BF_4); PF_6 , **9a**(PF_6); $\text{Al}\{\text{OC}(\text{CF}_3)_3\}_4$, **9a**(AIR^{F_4})) and $[(\eta^3\text{-C}_3\text{H}_5)\text{Pd}\{\text{C}(\text{N}(\text{C}_6\text{H}_3\text{-}2,6\text{-iPr}_2)\text{CH}_2)\}(\text{THF})]\text{Y}$ (Y = BF_4 , **9c**(BF_4); PF_6 , **9c**(PF_6)) and the CH_2Cl_2 -solvates $[(\eta^3\text{-C}_3\text{H}_5)\text{Pd}\{\text{C}(\text{N}(\text{tBu})\text{CH}_2)\}(\text{CH}_2\text{Cl}_2)]\text{AIR}^{\text{F}_4}$ (**11a**(AIR^{F_4})) and $[(\eta^3\text{-C}_3\text{H}_5)\text{Pd}\{\text{C}(\text{N}(\text{C}_6\text{H}_3\text{-}2,6\text{-iPr}_2)\text{CH}_2)\}(\text{CH}_2\text{Cl}_2)]\text{PF}_6 \cdot 2\text{CH}_2\text{Cl}_2$ (**11c**(PF_6)) have been isolated. In contrast, reaction of **6a,c** with AgBF_4 in toluene or CH_2Cl_2 yields the neutral solvent-free BF_4 adducts $(\eta^3\text{-C}_3\text{H}_5)\text{Pd}\{\text{C}(\text{N}(\text{tBu})\text{CH}_2)\}(\text{BF}_4)$ (**12a**) and $(\eta^3\text{-C}_3\text{H}_5)\text{Pd}\{\text{C}(\text{N}(\text{C}_6\text{H}_3\text{-}2,6\text{-iPr}_2)\text{CH}_2)\}(\text{BF}_4)$ (**12c**), consistent with the marked nucleophilicity of the BF_4 anion. Drying the CH_2Cl_2 -solvates **11a,c**(Y) (Y = PF_6 , AIR^{F_4}) at ambient temperature under vacuum affords the PF_6 and AIR^{F_4} adducts $(\eta^3\text{-C}_3\text{H}_5)\text{Pd}\{\text{C}(\text{N}(\text{tBu})\text{CH}_2)\}(\text{PF}_6)$ (**13a**), $(\eta^3\text{-C}_3\text{H}_5)\text{Pd}\{\text{C}(\text{N}(\text{C}_6\text{H}_3\text{-}2,6\text{-iPr}_2)\text{CH}_2)\}(\text{PF}_6)$ (**13c**), $(\eta^3\text{-C}_3\text{H}_5)\text{Pd}\{\text{C}(\text{N}(\text{tBu})\text{CH}_2)\}(\text{AIR}^{\text{F}_4})$ (**14a**), and $(\eta^3\text{-C}_3\text{H}_5)\text{Pd}\{\text{C}(\text{N}(\text{C}_6\text{H}_3\text{-}2,6\text{-iPr}_2)\text{CH}_2)\}(\text{AIR}^{\text{F}_4})$ (**14c**). Reaction of **8–14** with water produces the (nonisolated) water adducts $[(\eta^3\text{-C}_3\text{H}_5)\text{Pd}(\text{NHC})(\text{H}_2\text{O})]\text{Y}$ (**10a–d**(Y)). The molecular structures of **5a**, **9a**(BF_4), **11c**(PF_6), and **12a** have been determined. The various anions and solvate ligands are arranged in their order of donor strength/nucleophilicity toward the $[(\pi\text{-allyl})\text{Pd}(\text{NHC})]^+$ moiety.

Introduction

There is an enduring interest in the synthesis and properties of formally ionic three-coordinate $14e$ complexes of the type $[(\eta^3\text{-C}_3\text{H}_5)\text{M}(\text{L})]\text{Y}$ (M = Ni, Pd), in which L is a monodentate donor ligand such as a phosphine or, more recently, N-heterocyclic carbene ligand (NHC) and Y is a noncoordinating or very weakly coordinating anion. These efforts originate from Wilke's seminal studies on the activation of $(\eta^3\text{-C}_3\text{H}_5)\text{Ni}(\text{PR}_3)\text{X}$ complexes (X = halide) with Lewis acids $\text{AIR}'_n\text{X}_{3-n}$, which give rise to isolable adducts $(\eta^3\text{-C}_3\text{H}_5)\text{Ni}(\text{PR}_3)(\mu\text{-X})\text{AIR}'_n\text{X}_{3-n}$ (**1a**),¹ of which $(\eta^3\text{-C}_3\text{H}_5)\text{Ni}(\text{PCy}_3)(\mu\text{-Cl})\text{AlMeCl}_2$ has been characterized by X-ray structure analysis.² Complexes of this type are active catalysts for the dimerization of propene, the highest activity paired with the highest selectivity being observed for a $\text{P}^i\text{Bu}^i\text{Pr}_2$ -modified catalyst.¹

Other important reactions involving the $(\eta^3\text{-allyl})\text{M}(\text{PR}_3)\text{X}$ unit (M = Ni, Pd) are the $(\eta^3\text{-allyl})\text{Ni}(\text{P}^i\text{Pr}_3)\text{X}/\text{AgY}$ (Y = BF_4 ,

ClO_4 , CF_3SO_3)-catalyzed cyclization of 1,5- and 1,6-dienes,³ the nickel-catalyzed hydrovinylation of vinylarenes, cyclic 1,3-dienes, and norbornene,⁴ and the $(\eta^3\text{-C}_3\text{H}_5)\text{Ni}(\text{PMe}_3)\text{Cl}/\text{AgBF}_4$ -catalyzed dimerization of methylacrylate.⁵ In the latter case the formation of intermediate $(\eta^3\text{-C}_3\text{H}_5)\text{Ni}(\text{PMe}_3)\text{BF}_4$ (**1b**) has been proposed, which is closely related to **1a**. Japanese authors have reported a $(\eta^3\text{-C}_3\text{H}_5)\text{Pd}(\text{PR}_3)\text{Cl}/\text{AgY}$ or TiY (Y = e.g., BF_4 , PF_6 , SbF_6 , ClO_4)-catalyzed coupling of vinylarenes with terminal alkenes. They presume that the complex anion leaves an uncoordinated site at palladium.⁶ Widenhofer et al. have suggested that the 1,6-diene cycloisomerization catalyst generated by reaction of $(\eta^3\text{-C}_3\text{H}_5)\text{Pd}(\text{PCy}_3)\text{Cl}$ with NaBARF ($\text{BARF} = \text{B}\{\text{C}_6\text{H}_3\text{-}3,5\text{-(CF}_3)_2\}_4$) and HSiEt_3 in CH_2Cl_2 contains a potential vacant coordination site on palladium that could be occupied by some weakly coordinated ligand such as solvent, water, or silane.⁷ Brookhart and others have protolyzed $(\eta^3\text{-}$

(3) Bogdanovic, B.; Galle, J.; Hoffman, N.; Wilke, G. Unpublished (1972–1974). Cited in ref 1e, pp 113 and 127.

(4) (a) See ref 1f. (b) Jolly, P. W.; Wilke, G. Hydrovinylation. In *Applied Homogeneous Catalysis with Organometallic Compounds*; Cornils, B., Herrmann, W. A., Eds.; VHC: New York, 1996; Vol. 2, pp 1024–1048. (c) Jin, J.; RajanBabu, T. V. *Tetrahedron* **2000**, *56*, 2145. Kumareswaran, R.; Nandi, M.; RajanBabu, T. V. *Org. Lett.* **2003**, *5*, 4345.

(5) (a) Sperling, K. Dissertation (G. Wilke), Universität Bochum, Germany, 1983. (b) Wilke, G.; Sperling, K.; Stehling, L. German Patent DOS 3.336.691; US Patent 4.594.1983447, 1986. (c) Wilke, G. *Proc. 5th IUPAC Symp. Org. Synth.* **1984**; Blackwell: Oxford, 1985; p 1. (d) Ref 1f.

(6) Hattori, S.; Munakata, H.; Tatsuoka, K.; Shimizu, T. US Patent 3.803.254, 1974.

(1) (a) Birkenstock, U.; Bönemann, H.; Bogdanovic, B.; Walter, D.; Wilke, G. *Adv. Chem. Ser.* **1968**, *70*, 250. (b) Bogdanovic, B.; Wilke, G. *Brennstoff-Chemie* **1968**, *49*, 323. (c) Bogdanovic, B.; Henc, B.; Karmann, H.-G.; Nüssel, H.-G.; Walter, D.; Wilke, G. *Ind. Eng. Chem.* **1970**, *62* (12), 34. (d) Bogdanovic, B.; Henc, B.; Lösler, A.; Meister, B.; Pauling, H.; Wilke, G. *Angew. Chem.* **1973**, *85*, 1013; *Angew. Chem., Int. Ed. Engl.* **1973**, *12*, 954. (e) Bogdanovic, B. *Adv. Organomet. Chem.* **1979**, *17*, 105. (f) Wilke, G. *Angew. Chem.* **1988**, *100*, 189; *Angew. Chem., Int. Ed. Engl.* **1988**, *27*, 185.

(2) Bogdanovic, B.; Ilmaier, B.; Walter, D.; Wilke, G.; Krüger, C.; Tsay, Y.-H. 1972. Cited in ref 1d, Figure 3.

$C_3H_5Pd(PR_3)Me$ ($R = nBu, Cy$) with $[H(OEt_2)_2]BARF$ to isolate the ionic solvate complexes $[(\eta^3-C_3H_5)Pd(PR_3)(OEt_2)]BARF$ (**2**).⁸

In addition, a series of dimeric complexes $\{(\eta^3\text{-allyl})M(\mu\text{-}O_2CR)\}_2$ ($M = Ni, Pd; R = CH_3, CF_3$) (**3a**)⁹ with bridging acetate or trifluoroacetate groups have been isolated, of which $\{(\eta^3-C_3H_5)Pd(\mu\text{-}O_2CCH_3)\}_2$ ^{9a} and $\{(\eta^3\text{-}2\text{-}MeC_3H_4)M(\mu\text{-}O_2\text{-}CCF_3)\}_2$ (isostructural for $M = Ni$ and Pd)^{9c} have been characterized by X-ray structure analysis. $\{(\eta^3-C_3H_5)Pd(\mu\text{-}BF_4)\}_2$ (**3b**) and $\{(\eta^3-C_3H_5)Pd(\mu\text{-}SbF_6)\}_2$ (**3c**) prepared in situ are reported to decompose on attempting to isolate them.¹⁰

Using NHC ligands, Nolan et al. have shown that reaction of neutral halide complexes $(\eta^3-C_3H_5)Pd(NHC)Cl$ with AgY ($Y = BF_4, PF_6$) in acetonitrile affords cationic solvent adducts $[(\eta^3-C_3H_5)Pd(NHC)(NCMe)]Y$, whereas the products generated in THF were considered unstable.^{11a} Although the acetonitrile-containing complexes have been repeatedly referred to as $(IPr)Pd(allyl)BF_4$ and $(IPr)Pd(allyl)PF_6$ ($IPr = C(N(C_6H_3\text{-}2,6\text{-}iPr_2)CH_2)_2$), there is so far no compelling evidence that the latter species actually exist. Related complexes $[(\eta^3-C_3H_5)Ni(NHC)(L)]BARF$, isolated for $L = H_2O$ and $MeCN$, have been reported most recently.^{11b} Interestingly, in an ionic $[(\eta^3\text{-allyl})Pd(NHC)]BF_4$ complex bearing an extensive NHC ligand the cation is stabilized by an agostic $Pd\cdots H$ interaction.¹²

Attempts to prepare PF_6 salts by reaction with commercial $AgPF_6$ have frequently resulted in the isolation of F_2PO_2 complexes.^{13a–f} Although the mechanisms of the reactions remain obscure, it seems reasonable to assume that a transition metal-assisted hydrolysis of the PF_6 anion by moisture contained in either the reagent or the solvent occurred to afford the difluorophosphate. Reaction of $((\eta^3\text{-}MeC_3H_4)PdCl)_2$ with $AgPF_6$ and water gives the trimer $\{(\eta^3\text{-}MeC_3H_4)Pd(\mu\text{-}O_2PF_2)\}_3$ (**3d**), which reacts with PCy_3 to afford $(\eta^3\text{-}MeC_3H_4)Pd(PCy_3)(O_2PF_2)$.^{13g}

Our early attempts to synthesize $[(\eta^3-C_3H_5)M(L)]Y$ ($M = Ni, Pd; L = PR_3$ or NHC) complexes from the halides $(\eta^3-C_3H_5)M(L)X$ ($X = Cl, Br, I$) by halide abstraction with TiY or AgY reagents resulted in the formation of the novel cationic,

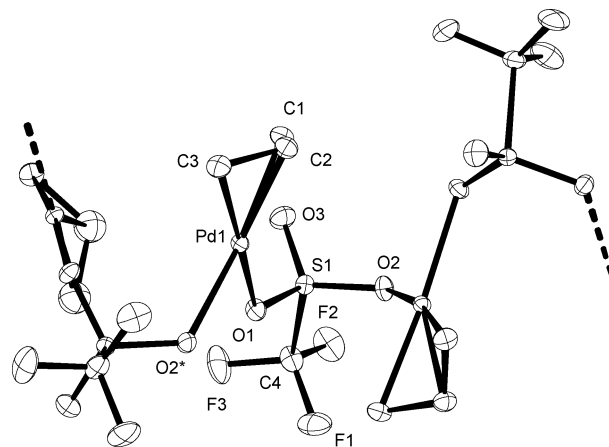
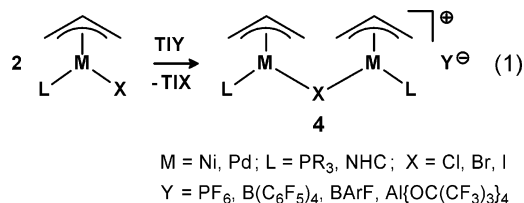


Figure 1. Molecular structure of **5a** in the crystal. For data of the structure analysis, see Table S1 of the Supporting Information. Selected bond distances (Å), angles (deg), and torsion angles (deg): Pd1–C1 = 2.110(2), Pd1–C2 = 2.107(2), Pd1–C3 = 2.102(2), Pd1–O1 = 2.176(1), Pd1–O2* = 2.185(1), C1–C2 = 1.409(2), C2–C3 = 1.401(2); O1–Pd1–O2* = 85.94(4), C1–Pd1–O2* = 168.8(1), C3–Pd1–O1 = 171.4(1); O2*–Pd1–O1–S1 = –168.0(1), Pd1–O1–S1–O2 = 71.6(1), O1–S1–O2–Pd1** = –13.2(1), S1–O2–Pd1**–O1** = –109.2(1).

single halide-bridged metal-pair complexes $\{[(\eta^3-C_3H_5)M(L)]_2(\mu\text{-}X)]Y$ (**4**) ($Y = PF_6, B(C_6F_5)_4, BARF, AlR^F_4$) (eq 1).^{14,15} For the synthesis of pure **4** TiY can be used in a stoichiometric



amount (1/2 equiv) or in excess, while with AgY the stoichiometric quantity has to be used for best results. Due to the easy formation of complexes **4**, it can be expected that at least in some of the reactions cited above similar dinuclear complexes might have been generated unnoticed.

Our continuing efforts focused on palladium complexes with NHC ligands and using AgY reagents has now led to the isolation of mononuclear complexes $[(\eta^3-C_3H_5)Pd(NHC)\text{-}(solvent)]Y$ (solvent = Et_2O, THF, CH_2Cl_2) and $(\eta^3-C_3H_5)Pd(NHC)Y$ ($Y = BF_4, PF_6, AlR^F_4$), of which the examples $[(\eta^3-C_3H_5)Pd\{C(N^iBu)CH_2\}_2](THF)]BF_4$, $(\eta^3-C_3H_5)Pd\{C(N^iBu)CH_2\}_2(BF_4)$, and $[(\eta^3-C_3H_5)Pd\{C(N(C_6H_3\text{-}2,6\text{-}iPr_2)CH_2)\}_2](CH_2Cl_2)]PF_6$ have been structurally characterized.

Results

$\{(\eta^3\text{-allyl})Pd(\mu\text{-}OTf)\}_n$ (**5**). To begin with we should like to point out that the reaction of $\{(\eta^3-C_3H_5)Pd(\mu\text{-}Cl)\}_2$ with $AgOTf$ in diethyl ether (20 °C) yields the yellow polymeric triflate complex $\{(\eta^3-C_3H_5)Pd(\mu\text{-}OTf)\}_n$ (**5a**) (eq 2).¹⁶ The high solubility of **5a** in diethyl ether and THF suggests that the polymeric structure breaks down by solvation. Considering that **5a** crystallizes from the diethyl ether solution in the cold without inclusion of solvent, one might conclude that the coordinative

(14) (a) Alberti, D.; Goddard, R.; Pörschke, K.-R. *Organometallics* **2005**, *24*, 3907. (b) Ding, Y.; Goddard, R.; Pörschke, K.-R. *Organometallics* **2005**, *24*, 439.

(15) Such complexes have also been the subject of a patent. Goodall, B. L.; Petoff, J. L.; Shen, H. US Patent Application 2005/0043494 A1.

(7) (a) Widenhoefer, R. A.; Perch, N. S. *Org. Lett.* **1999**, *1*, 1103. (b) Kisanga, P.; Widenhoefer, R. A. *J. Am. Chem. Soc.* **2000**, *122*, 10017. (c) Widenhoefer, R. A. *Acc. Chem. Res.* **2002**, *35*, 905.

(8) (a) DiRenzo, G. M.; White, P. S.; Brookhart, M. J. *Am. Chem. Soc.* **1996**, *118*, 6225. (b) Lipian, J.; Mimna, R. A.; Fondran, J. C.; Yandulov, D.; Shick, R. A.; Goodall, B. L.; Rhodes, L. F.; Huffman, J. C. *Macromolecules* **2002**, *35*, 8969.

(9) (a) Robinson, S. D.; Shaw, B. L. *J. Organomet. Chem.* **1965**, *3*, 367. Churchill, M. R.; Mason, R. *Nature* **1964**, *204*, 777. (b) Powell, J. J. *Am. Chem. Soc.* **1969**, *91*, 4311. (c) Brown, R. G.; Chaudhari, R. V.; Davidson, J. M. *J. Chem. Soc., Dalton Trans.* **1977**, 176. (d) Vitagliano, A.; Åkermark, B.; Hansson, S. *Organometallics* **1991**, *10*, 2592. (e) Goddard, R.; Krüger, C.; Mynott, R.; Neumann, M.; Wilke, G. *J. Organomet. Chem.* **1993**, *454*, C20.

(10) (a) Reinmuth, A.; Mathew, J. P.; Melia, J.; Risse, W. *Macromol. Rapid Commun.* **1996**, *17*, 173. (b) Mathew, J. P.; Reinmuth, A.; Melia, J.; Swords, N.; Risse, W. *Macromolecules* **1996**, *29*, 2755.

(11) (a) Viciu, M. S.; Zinn, F. K.; Stevens, E. D.; Nolan, S. P. *Organometallics* **2003**, *22*, 3175. (b) Cámpora, J.; de la Tabla, L. O.; Palma, P.; Alvarez, E.; Lahoz, F.; Mereiter, K. *Organometallics* **2006**, *25*, 3314.

(12) Lavallo, V.; Canac, Y.; DeHope, A.; Donnadiou, B.; Bertrand, G. *Angew. Chem., Int. Ed.* **2005**, *44*, 7236.

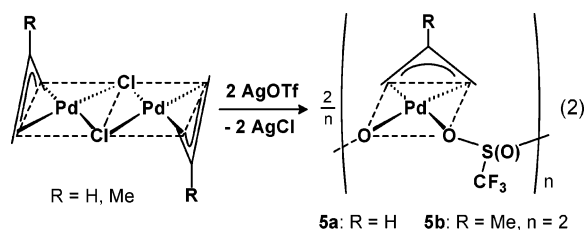
(13) (a) Thompson, S. J.; Bailey, P. M.; White, C.; Maitlis, P. M. *Angew. Chem., Int. Ed.* **1976**, *15*, 490. White, C.; Thompson, S. J.; Maitlis, P. M. *J. Organomet. Chem.* **1977**, *137*, 319. (b) Wimmer, F. L.; Snow, M. R. *Aust. J. Chem.* **1978**, *31*, 267. (c) Horn, E.; Snow, M. R. *Aust. J. Chem.* **1980**, *33*, 2369. (d) Smith, G.; Cole-Hamilton, D. J.; Gregory, A. C.; Gooden, N. G. *Polyhedron* **1982**, *1*, 97. (e) Bauer, H.; Nagel, U.; Beck, W. *J. Organomet. Chem.* **1985**, *290*, 219. (f) Bruno, G.; Schiavo, S. L.; Piraino, P.; Faraone, F. *Organometallics* **1985**, *4*, 1098. (g) Fernández-Galán, R.; Manzano, B. R.; Otero, A.; Lanfranchi, M.; Pellinghelli, M. A. *Inorg. Chem.* **1994**, *33*, 2309.

Table 1. Allyl NMR Data for the $\{(\eta^3\text{-}2\text{-RC}_3\text{H}_4)\text{Pd}(\mu\text{-OTf})\}_n$ Complexes **5a,b** and for Reference Compounds^a

	$\delta(^1\text{H})$			$\delta(^{13}\text{C})$		
	CH/Me	CH ₂ (syn)	CH ₂ (anti)	CH/Me	CH ₂	Me
$\{(\text{C}_3\text{H}_5)\text{Pd}(\mu\text{-Cl})\}_2$	5.40	4.05	2.98	111.1	62.9	
$\{(\text{C}_3\text{H}_5)\text{Pd}(\mu\text{-OTf})\}_n$ (5a) ^b	5.72	4.37	3.20	113.8	64.6	
$\{(\text{C}_3\text{H}_5)\text{Pd}(\mu\text{-BF}_4)\}_2$ (3a) ^{10b}	5.93	4.64	3.52	116.2	67.0	
$\{(\text{C}_3\text{H}_5)\text{Pd}(\mu\text{-SbF}_6)\}_2$ (3b) ^{10b}	6.08	4.87	3.74	118.5	70.4	
$\{2\text{-MeC}_3\text{H}_4\text{Pd}(\mu\text{-Cl})\}_2$	2.13	3.85	2.88	127.0	61.8	22.7
$\{2\text{-MeC}_3\text{H}_4\text{Pd}(\mu\text{-OTf})\}_2$ (5b) ^c	2.24	4.08	2.98	130.7	60.4	22.4

^a Solvent CD₂Cl₂. Temperature 25 °C. ^bOTf: $\delta(\text{C})$ 120.9, $J(\text{CF}) = 319$ Hz. ^cOTf: $\delta(\text{C})$ 119.9, $J(\text{CF}) = 318$ Hz.

bonds of the Et₂O and $\mu\text{-OTf}$ ligands to Pd are about equal in strength. **5a** dissolves only sparingly in CH₂Cl₂ or toluene. In contrast to the synthesis and properties of **5a**, $\{(\eta^3\text{-}2\text{-MeC}_3\text{H}_4)\text{Pd}(\mu\text{-Cl})\}_2$ is best reacted with AgOTf in CH₂Cl₂ or toluene to give, after separation of AgCl, a yellow solution, from which yellow needles of the methallyl derivative **5b** separate (eq 2). Because of the high solubility of **5b** in the non- (or weakly) coordinating solvents, we assume that it has a dimeric structure ($n = 2$), analogous to **3a**. Dissolving **5b** in diethyl ether gives rise to a weak solvent adduct $(\eta^3\text{-}2\text{-MeC}_3\text{H}_4)\text{Pd}(\text{Et}_2\text{O})\text{OTf}$, which slowly loses Et₂O when drying under vacuum at room temperature.



Complexes **5a,b** are thermally quite stable and can be kept at ambient temperature as solids and in solution. In the EI mass spectra of **5a** (135 °C) and **5b** (115 °C) the ions of both the mono- and dinuclear molecular entities are found in notable abundance, suggesting that the complexes evaporate preferably as dimers. The complexes are related to the structurally characterized M-allyl complexes **3a** (dimeric) and **3d** (trimeric) with $\mu\text{-O}_2\text{CR}$ or $\mu\text{-O}_2\text{PF}_2$ ligands and also to **3b,c** prepared in situ with the even weaker donating $\mu\text{-BF}_4$ and $\mu\text{-SbF}_6$ ligands, which are also anticipated to have dinuclear structure. The upfield solution ¹H and ¹³C NMR chemical shift of the allyl group in complexes $\{(\eta^3\text{-}2\text{-RC}_3\text{H}_4)\text{PdX}\}_n$ reflects nicely an increasing donor strength of X toward Pd in the series $\text{SbF}_6 < \text{BF}_4 < \text{OTf} < \text{Cl}$ (Table 1), so that the donor strength of OTf appears stronger than that of $\mu\text{-BF}_4$, but weaker than that of $\mu\text{-Cl}$.

In contrast to the dimeric carboxylates **3a**, the triflate **5a** comprises in the crystal close-packed infinite chains of $(\eta^3\text{-C}_3\text{H}_5)\text{Pd}$ cationic species bridged via the O atoms of interstitial anionic triflate moieties. Figure 1 shows a view perpendicular to one of the chains. C1, C3, Pd1, O1, and O2* are coplanar (rms deviation: 0.04 Å), but because of different torsional angles of the two Pd–O bonds ($\text{O}2^*-\text{Pd}1-\text{O}1-\text{S}1 = -168.0(1)^\circ$ and $\text{S}1^*-\text{O}2^*-\text{Pd}1-\text{O}1 = -109.2(1)^\circ$), the coordination sphere around the Pd1 center is chiral. The unequal Pd–O distances of 2.176(1) and 2.185(1) Å are smaller than in the dinuclear $\{(o\text{-tol})_3\text{PPd}(\text{Me})(\mu\text{-OTf})\}_2$ (2.19, 2.24 Å)¹⁷ as the only other

Pd(II) complex¹⁸ having bridging OTf ligands, and they fall into the range otherwise typically observed for Pd complexes with nonbridging triflate ligands (2.12–2.20 Å).¹⁹ The chains form chiral helices with three molecular subunits making up one helix turn. The helix has a pitch of 10.048(1) Å, and the coordination planes of adjacent Pd atoms make angles of 41° to one another. The long Pd···Pd distance of 3.460(1) Å indicates that metal–metal interactions do not make a strong contribution to the stabilization of the helix.

When treated with donor ligands L, the easily available and stable triflate complexes **5a,b** readily undergo cleavage of the $\mu\text{-OTf}$ bridges and thus represent valuable starting compounds for the synthesis of mononuclear adducts $(\eta^3\text{-}2\text{-RC}_3\text{H}_4)\text{Pd}(\text{L})\text{OTf}$.

$(\eta^3\text{-allyl})\text{Pd}(\text{NHC})\text{Me}$ (**7**) and $(\eta^3\text{-allyl})\text{Pd}(\text{NHC})(\text{OTf})$ (**8**). Previously we have presented preliminary results on the formation and properties of the mononuclear neutral methyl and triflate complexes $(\eta^3\text{-allyl})\text{Pd}(\text{NHC})\text{Me}$ (**7**) and $(\eta^3\text{-allyl})\text{Pd}(\text{NHC})(\text{OTf})$ (**8**).^{14b} Reaction of the chlorides $(\eta^3\text{-}2\text{-RC}_3\text{H}_4)\text{Pd}(\text{NHC})\text{Cl}$ (R = H, Me) (**6a–d**)^{20,21} with (tmeda)MgMe₂²² affords the PdCH₃ derivatives **7a–d** (eq 3a). The more robust aryl-substituted **7c,d** can also be synthesized using LiMe. While **7c** has been previously prepared by us,^{14b} **7a,b** and **7d** are new.

7a–d have been crystallized from pentane. The complexes are thermally quite stable. According to DSC **7a,b** undergo irreversible endothermic transformations at about 90 °C, while **7c,d** decompose exothermically at 130 °C. In the EI mass spectra of **7a–d** the molecular ions are detected (1–2%), which fragment by loss of the methyl group to give $[(\text{allyl})\text{Pd}(\text{NHC})]^+$

(17) Yamashita, M.; Takamiya, I.; Jin, K.; Nozaki, K. *Organometallics* **2006**, *25*, 4588.

(18) For Pd(I)–Pd(I) complexes with triflate bridges having substantially longer Pd–O bonds (2.28–2.32 Å), see: (a) Leoni, P.; Pasquali, M.; Sommovigo, M.; Albinati, A.; Lianza, F.; Pregosin, P. S.; Rüegger, H. *Organometallics* **1993**, *12*, 4503. (b) Leoni, P.; Vichi, E.; Lencioni, S.; Pasquali, M.; Chiarentin, E.; Albinati, A. *Organometallics* **2000**, *19*, 3062.

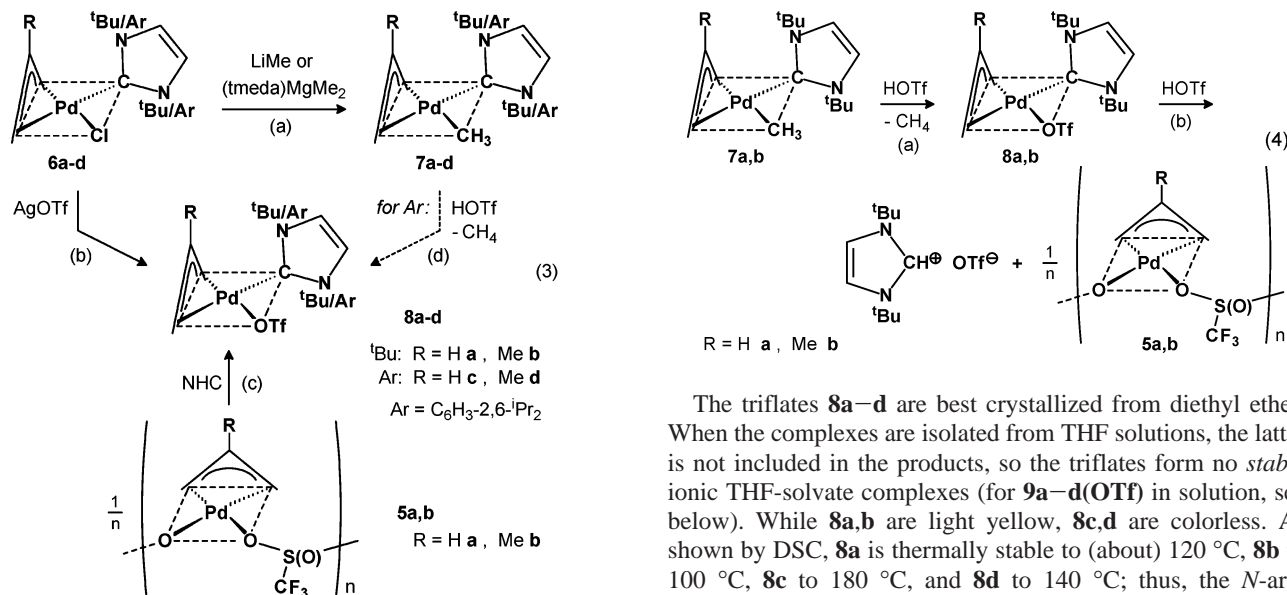
(19) (a) Burger, P.; Baumeister, J. M. *J. Organomet. Chem.* **1999**, *575*, 214. (b) Müller, T. E.; Berger, M.; Grosche, M.; Herdtweck, E.; Schmidchen, F. P. *Organometallics* **2001**, *20*, 4384. (c) Vicente, J.; Abad, J.-A.; Martínez-Viviente, E.; Jones, P. G. *Organometallics* **2002**, *21*, 4454. (d) Ref 8b. (e) Burrows, A. D.; Mahon, M. F.; Varrone, M. *J. Chem. Soc., Dalton Trans.* **2003**, 4718. (f) Stambuli, J. P.; Incarvito, C. D.; Bühl, M.; Hartwig, J. F. *J. Am. Chem. Soc.* **2004**, *126*, 1184. (g) Lu, C. C.; Peters, J. C. *J. Am. Chem. Soc.* **2004**, *126*, 15818.

(20) (a) Caddick, S.; Cloke, F. G. N.; Clentsmith, G. K. B.; Hitchcock, P. B.; McKerrecher, D.; Titcomb, L. R.; Williams, M. R. V. *J. Organomet. Chem.* **2001**, *617–618*, 635. (b) Navarro, O.; Oonishi, Y.; Kelly, R. A.; Stevens, E. D.; Briel, O.; Nolan, S. P. *J. Organomet. Chem.* **2004**, *689*, 3722.

(21) (a) Viciu, M. S.; Germaneau, R. F.; Navarro-Fernandez, O.; Stevens, E. D.; Nolan, S. P. *Organometallics* **2002**, *21*, 5470. (b) Viciu, M. S.; Navarro, O.; Germaneau, R. F.; Kelly, R. A., III; Sommer, W.; Marion, N.; Stevens, E. D.; Cavallo, L.; Nolan, S. P. *Organometallics* **2004**, *23*, 1629.

(22) (a) We have noted before the superior methylating properties of (tmeda)MgMe₂ compared to LiMe: Kaschube, W.; Pörschke, K.-R.; Wilke, G. *J. Organomet. Chem.* **1988**, *355*, 525. (b) For the synthesis and properties of (tmeda)MgMe₂, see: Kaschube, W.; Pörschke, K.-R.; Angermund, K.; Krüger, C.; Wilke, G. *Chem. Ber.* **1988**, *121*, 1921.

(16) For a Pd₂($\mu\text{-OTf}$)₂ complex having 2-dimethylaminomethylene-1-naphthyl ligands instead of the π -allyl groups, see: Valk, J.-M.; van Belzen, R.; Boersma, J.; Spek, A. L.; van Koten, G. *J. Chem. Soc., Dalton Trans.* **1994**, 2293.



as prominent ions (35–50%). In the ESIpos mass spectra of the aryl-substituted **7c,d** this ion ($m/e = 535$ and 549 , respectively) is a base peak and almost solely observed. In contrast, for the ^tBu-substituted **7a,b** the ions [(allyl)Pd(NHC)]⁺ (m/e 327 and 341), formed after cleavage of Me from M⁺, and [(NHC)PdMe]⁺ (m/e 301), formed after cleavage of allyl from M⁺, appear in about equal moderate intensity. The base ion is [MeC(N(^tBu)CH)₂]⁺ (m/e 195), generated by transfer of the methyl group to the NHC. The NMR spectra of **7a–d** are discussed below.

When the chloride complexes **6a–d** are reacted with 1 equiv of AgOTf, AgCl is eliminated and the mononuclear triflate complexes **8a–d** are formed (eq 3b). The reaction is remarkable in view of the fact that previous attempts to react the iodides with 1 equiv of AgOTf or to react either chlorides or iodides with TlOTf resulted only in partial halide substitution and formation of the dinuclear complexes **4**. While the NHC ligand at Pd is not transferred to AgCl although (NHC)AgCl complexes are stable,²³ the NHC ligand does transfer to an excess of the AgY reagent with formation of (NHC)AgY (Y = e.g., OTf, BF₄, PF₆). Therefore, an excess of the AgY reagent must be avoided. Complexes **8a–d** are most easily obtained from **5a,b** by cleavage of the μ -OTf bridges with NHC (eq 3c). Furthermore, the aryl-substituted **8c,d** can be prepared by selective protolysis of the PdMe function in **7c,d** with HOTf (eq 3d).

In contrast, protolysis of the ^tBu-substituted **7a,b** with 1 equiv of HOTf at –40 °C results in the formation of substantial amounts of the imidazolium triflate and the NHC-free {(η^3 -2-RC₃H₄)Pd(μ -OTf)}_n (**5a,b**) (eq 4). When only 1/2 equiv of HOTf is used, part of **7a,b** can be recovered and some **8a,b** is formed, but no imidazolium triflate. We have shown in a separate experiment that **8a,b** react readily with HOTf at –40 °C by protonation of the C{N(^tBu)CH}₂ ligand to give the imidazolium triflate and **5a,b**. The findings suggest that **7a,b** indeed react with HOTf preferably by protolysis of the PdCH₃ function (and not by protonation of the C{N(^tBu)CH}₂ ligand) to give intermediates **8a,b**, but the latter reacts as readily further with the acid by protonation of the C{N(^tBu)CH}₂ ligand to yield **5a,b** and the imidazolium triflate. Hence, protolysis of **7a,b** is not suited for the synthesis of **8a,b**.

The triflates **8a–d** are best crystallized from diethyl ether. When the complexes are isolated from THF solutions, the latter is not included in the products, so the triflates form no *stable* ionic THF-solvate complexes (for **9a–d(OTf)** in solution, see below). While **8a,b** are light yellow, **8c,d** are colorless. As shown by DSC, **8a** is thermally stable to (about) 120 °C, **8b** to 100 °C, **8c** to 180 °C, and **8d** to 140 °C; thus, the *N*-aryl complexes are more stable than the *N*-^tBu complexes and the parent allyl complexes are somewhat more stable than the methallyl derivatives. In the EI mass spectra of **8a–d** the molecular ions and [(allyl)Pd(NHC)]⁺ are observed in about equal intensity (1–7%). In the ESIpos mass spectra of **8a–d** [(allyl)Pd(NHC)]⁺ represents the base peak, as for **7c,d**.

The ¹H and ¹³C NMR data of the various (allyl)Pd(NHC)X complexes **7a–d** and **8a–d** in CD₂Cl₂ and THF-*d*₈ are listed for the parent allyl methyl and triflate complexes in Table 2 (NHC = C(N(^tBu)CH)₂; **7a, 8a**) and Table 3 (NHC = C(N(C₆H₃-2,6-ⁱPr₂)CH)₂; **7c, 8c**) and for the methallyl derivatives in Tables S2 (**7b, 8b**) and S3 (**7d, 8d**) of the Supporting Information. In addition, the chemical shifts of the π -allyl groups are represented schematically in Figures 2, 3, S2, and S3, including the data of the corresponding chlorides. A similar evaluation was previously performed for (η^3 -C₃H₅)Pd(PⁱPr₃)X complexes (see ref 24, Figures 1 and 2), which in turn was preceded inter alia by a ¹³C NMR study on related complexes with substituted allyl groups.²⁵ For the complexes with phosphorus ligands it was possible to assign the ¹H and ¹³C resonances of the allyl methylene groups on the basis of the marked couplings to the trans phosphorus ligand. Since many features of the allyl NMR resonances of the NHC complexes are very similar to those of the PⁱPr₃ complexes,²⁴ the assignment of the allyl resonances of the NHC complexes can be based on that of the PⁱPr₃ complexes.

We first note that the ¹H and ¹³C NMR spectra of the *methyl complexes 7a–d* in CD₂Cl₂ and THF-*d*₈ are independent of the solvent and the temperature between –80 and 25 °C. The spectra are in agreement with rigid C₁ symmetrical structures of the complexes; that is, neither π - σ -allyl isomerization nor ligand dissociation occurs at ambient temperature. Fully resolved spectra are also observed for the *chlorides 6a–d* at ambient temperature in CD₂Cl₂ solution, whereas in THF-*d*₈ some line-broadening of H1a and H1s indicates an incipient selective π - σ -allyl isomerization.^{24,26} In **6a,b** and **7a,b** the bulk of the two

(24) Krause, J.; Goddard, R.; Mynott, R.; Pörschke, K.-R. *Organometallics* **2001**, *20*, 1992.

(25) Åkermark, B.; Krakenberger, B.; Hansson, S.; Vitagliano, A. *Organometallics* **1987**, *6*, 620.

(26) (a) Vrieze, K. In *Dynamic Nuclear Magnetic Resonance Spectroscopy*; Jackman, L. M., Cotton, F. A., Eds.; London: Academic Press, 1975; pp 441–487, see p 454. (b) Crociani, B.; Antonaroli, S.; Bandoli, G.; Canovesi, L.; Visentin, F.; Uguagliati, P. *Organometallics* **1999**, *18*, 1137, and references therein. (c) Camus, J.-M.; Andrieu, J.; Richard, P.; Poli, R. *Eur. J. Inorg. Chem.* **2004**, 1081, and references therein.

(23) de Frémont, P.; Scott, N. M.; Stevens, E. D.; Ramnial, T.; Lightbody, O. C.; Macdonald, C. L. B.; Clyburne, J. A. C.; Abernethy, C. D.; Nolan, S. P. *Organometallics* **2005**, *24*, 6301.

Table 2. ^1H and ^{13}C NMR Data for the $(\eta^3\text{-C}_3\text{H}_5)\text{Pd}(\text{N}(\text{tBu})\text{CH})_2\text{X}$ Complexes **6a–11a(Y)**^a

	solvent	T, °C	allyl									C(N(tBu)CH) ₂					
			$\delta(\text{H})$					$\delta(\text{C})$				$\delta(\text{H})$			$\delta(\text{C})$		
			H2	H3s	H1s	H3a	H1a	C2	C3	C1	NCH	^t Bu	PdC	NCH	CMe ₃	Me	
6a	CD ₂ Cl ₂	25	5.30	4.04	3.41	3.24	2.30	112.8	68.9	52.3	7.22, 7.20	1.88, 1.72	177.5	118.8, 118.3	58.9, 58.8	32.2, 31.9	
6a	THF- <i>d</i> ₈	25	5.23	3.87	3.29	3.11	2.20	112.6	67.7	51.6	7.38, 7.36	1.89, 1.72	178.6	119.2, 118.9	59.0deg	32.1, 31.9	
7a^b	CD ₂ Cl ₂	25	4.94	2.84	3.20	2.18	2.14	114.1	47.5	59.8	7.16deg	1.72, 1.61	184.4	117.7, 117.2	58.2, 58.2	31.4, 31.1	
7a^c	THF- <i>d</i> ₈	25	4.88	2.78	3.15	2.14	2.08	114.4	47.5	59.8	7.30, 7.29	1.73, 1.62	n. d.	118.3, 117.7	58.4deg	31.4, 31.2	
8a	CD ₂ Cl ₂	-80	5.48	4.49	3.44	3.54	2.40	112.8	73.5	48.3	7.19, 7.16	1.79, 1.61	173.7	118.2, 117.4	57.9deg	31.2, 30.8	
8a	THF- <i>d</i> ₈	-80	5.65	4.48	3.42	3.60	2.51	114.1	73.7	48.4	7.64, 7.59	1.88, 1.69	174.7	120.1, 119.4	59.0, 58.9	31.9, 31.6	
9a(BF₄)^d	CD ₂ Cl ₂	-80	5.60	4.31	3.47	3.54	2.46	114.8	72.9	48.8	7.26, 7.23	1.78, 1.60	171.8	119.0, 118.2	58.1deg	31.0, 30.6	
9a(PF₆)^d	CD ₂ Cl ₂	-80	5.60	4.31	3.47	3.54	2.45	114.8	72.9	48.8	7.25, 7.23	1.79, 1.61	171.9	119.0, 118.2	58.1deg	31.1, 30.7	
9a(AIR^F₄)	CD ₂ Cl ₂	-80	data not available due to the low solubility of the complex														
9a(OTf)	THF- <i>d</i> ₈	-80	5.85	4.51	3.47	3.78	2.66	116.7	74.4	48.9	7.81, 7.75	1.90, 1.71	172.8	121.1, 120.4	59.3, 59.2	31.6, 31.4	
9a(BF₄)	THF- <i>d</i> ₈	-80	5.85	4.52	3.46	3.78	2.64	116.6	74.4	48.7	7.80, 7.74	1.90, 1.71	172.8	121.2, 120.5	59.3, 59.2	31.6, 31.4	
9a(PF₆)	THF- <i>d</i> ₈	-80	5.83	4.48	3.49	3.75	2.64	116.6	74.2	48.9	7.76, 7.72	1.90, 1.71	172.9	121.1, 120.3	59.3, 59.2	31.5, 31.3	
9a(AIR^F₄)	THF- <i>d</i> ₈	-80	5.83	4.46	3.52	3.74	2.67	116.7	73.9	49.1	7.79, 7.74	1.90, 1.72	172.9	121.1, 120.6	59.3, 59.2	31.4, 31.2	
10a(BF₄)	CD ₂ Cl ₂	-80	5.49	4.33	3.38	3.49	2.37	113.9	72.4	48.1	7.19, 7.17	1.77, 1.58	172.3	118.1, 117.5	57.9, 57.8	31.1, 30.7	
10a(PF₆)	CD ₂ Cl ₂	-80	5.54	4.33	3.46	3.52	2.44	114.2	72.6	48.6	7.20, 7.17	1.78, 1.60	171.9	118.4, 117.7	57.9, 57.9	31.3, 30.8	
10a(AIR^F₄)	CD ₂ Cl ₂	-80	5.56	4.29	3.53	3.50	2.51	114.4	72.3	49.4	7.20, 7.17	1.78, 1.60	171.6	118.7, 117.9	58.0, 58.0	31.2, 30.9	
10a(OTf)	THF- <i>d</i> ₈	-80	5.67	4.28	3.33	3.54	2.47	115.3	71.3	48.2	7.69, 7.63	1.87, 1.69	173.7	120.4, 119.7	59.0, 58.9	31.8, 31.5	
10a(BF₄)	THF- <i>d</i> ₈	-80	5.70	4.24	3.35	3.55	2.50	115.4	71.2	48.3	7.71, 7.65	1.88, 1.69	173.5	120.6, 119.9	59.1, 59.0	31.8, 31.5	
10a(PF₆)	THF- <i>d</i> ₈	-80	5.69	4.19	3.38	3.52	2.51	115.4	70.6	48.5	7.70, 7.64	1.88, 1.69	173.5	120.5, 119.8	59.1, 59.0	31.7, 31.4	
10a(AIR^F₄)	THF- <i>d</i> ₈	-80	5.72	4.21	3.39	3.52	2.52	115.9	70.7	48.8	7.73, 7.68	1.88, 1.69	173.8	120.3, 119.7	59.2, 59.1	31.7, 31.4	
11a(BF₄)	CD ₂ Cl ₂	-80	5.74	4.63	4.02	3.75	2.92	116.1	74.6	56.4	7.26	1.67	167.9	119.2	58.2	31.4	
11a(PF₆)	CD ₂ Cl ₂	-80	5.73	4.59	4.03	3.72	2.92	116.2	74.3	56.8	7.24	1.65	167.6	119.2	58.2	31.4	
11a(AIR^F₄)	CD ₂ Cl ₂	-80	5.71	4.54	4.05	3.70	2.93	116.1	73.9	56.9	7.23	1.65	167.3	119.2	58.2	31.3	

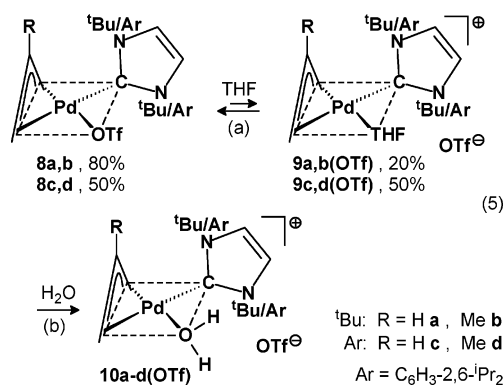
^a deg = degenerate. n.d. = not detected. R^F = OC(CF₃)₃. ^bPdCH₃: $\delta(\text{H})$ -0.15, $\delta(\text{C})$ -15.7. ^cPdCH₃: $\delta(\text{H})$ -0.17, $\delta(\text{C})$ -15.3. ^dTHF ligand: $\delta(\text{H})$ 3.61, 1.81; $\delta(\text{C})$ 75.5, 25.9.

^tBu groups impedes rotation of the C(N(^tBu)CH)₂ ligand about its Pd–C bond; therefore, the two N(^tBu)CH moieties of the NHC ligand are inequivalent and the corresponding resonances are duplicated (Tables 2 and S2). In contrast, in **6c,d** and **7c,d** both N(C₆H₃-2,6-ⁱPr₂)CH moieties of the C(N(C₆H₃-2,6-ⁱPr₂)-CH)₂ ligand are equivalent since the NCH ligand rotates about the Pd–C bond, as expected for a Fischer-type carbene complex. However, the aryl groups are fixed with respect to rotation about the N–C bonds, causing splitting of the ortho and meta aryl resonances. Due to the inequivalence of the ⁱPr substituents with diastereotopic Me groups, a total of four Me signals is found for the NHC ligand (Tables 3 and S3). The PdCH₃ NMR signals are unexceptional (e.g., **7a** in CD₂Cl₂: $\delta(\text{H})$ -0.15, $\delta(\text{C})$ -15.7).

The situation is more complicated for the triflate complexes **8a–d** since here the NMR spectra depend on both the solvent and the temperature. The ^1H and ^{13}C NMR spectra of **8a–d** in CD₂Cl₂ are only well-resolved at -80 °C (Tables 2, 3, S2, and S3) and evidence the presence of the undissociated complex with a rigid structure (like **6a–d** and **7a–d** at ambient temperature). However, in the ambient temperature spectra of **8a–d** in CD₂Cl₂ all allyl-proton and the allyl-C1/C3 resonances are broad and the NHC resonances are coalesced, indicative of a more complex allyl isomerization process and formal rotation of the NHC ligand.

Quite in contrast, the THF-*d*₈ solutions of **8a–d** at -80 °C show two sets of allyl and NHC signals for related rigid complexes, which are in a slow equilibrium. We assign the lower field signal set to the nonisolable cationic THF-solvates **9a–d(OTf)** and the higher field set to the neutral **8a–d** itself. For **8a–d** and further complexes a correlation of the isolated complexes and the species present in solution (which as such are listed in Tables 2, 3 S2, and S3) is given in Table 4. **8a** and its solvate derivatives (**9a(OTf)** and the water-solvate **10a(OTf)**, see below) have been studied in most detail. The low-field set assigned to **9a(OTf)** agrees well with the signals of the isolated THF-solvates **9a(Y)** (Y = BF₄, PF₆, AIR^F₄; Table 2) with the

same cation but different anions described below. For solutions of **8a,b** the undissociated complexes (that is, the actual **8a,b**) in fact represent the major component (80%) and the ionic THF-solvates **9a,b(OTf)** the minor component, without obvious concentration dependency of the solutions, whereas for solutions of the C(N(Ar)CH)₂-ligated **8c,d** the unaltered complexes and the THF-solvates **9c,d(OTf)** are present to about equal extent (eq 5a). Thus, the Pd–O bond strengths of the undissociated



Pd–OTf complexes **8a–d** and the cationic THF-solvates **9a–d** appear to be of similar magnitude, although dissociation (THF-solvate formation) seems to occur more readily for the C(N(Ar)-CH)₂-ligated (**8c,d**) than for the C(N(^tBu)CH)₂-ligated triflate complexes (**8a,b**). On the basis of the assumption of a similar donor strength of the OTf and THF ligands toward the $[(\eta^3\text{-allyl})\text{Pd}(\text{NHC})]^+$ moiety, the marked low-field shift of the resonances of the THF-solvates can be attributed to their cationic nature.

It seems worthy of note that in some of the NMR spectra of **8a,b** in THF-*d*₈ solution (-80 °C) we have even observed a third set of signals, which can be attributed to the water complexes **10a,b(OTf)**, resulting from traces of moisture present

Table 3. ^1H and ^{13}C NMR Data for the $(\eta^3\text{-C}_3\text{H}_5)\text{PdC}\{\text{N}(\text{C}_6\text{H}_3\text{-2,6-}^i\text{Pr}_2)\text{CH}\}_2\text{X}$ Complexes **6c**–**11c**(PF₆)^a

	solvent	T, °C	allyl							
			$\delta(\text{H})$					$\delta(\text{C})$		
			H2	H3s	H1s	H3a	H1a	C2	C3	C1
6c	CD ₂ Cl ₂	25	4.84	3.76	3.08	2.70	1.57	114.5	71.8	50.3
6c	THF- <i>d</i> ₈	25	4.77	3.61	3.04	2.58	1.55	114.1	70.8	49.6
7c^b	CD ₂ Cl ₂	25	4.52	2.56	3.00	1.70	1.40	115.4	49.3	58.9
7c^c	THF- <i>d</i> ₈	25	4.43	2.45	2.91	1.65	1.36	115.7	49.6	58.3
8c	CD ₂ Cl ₂	–80	5.02	4.29	2.93	3.16	1.63	115.2	79.0	44.8
8c	THF- <i>d</i> ₈	–80	5.22	4.23	3.01	3.28	1.77	116.5	79.7	44.9
9c(BF₄)^d	CD ₂ Cl ₂	–80	5.20	4.15	2.80	3.19	1.46	118.2	78.4	44.8
9c(PF₆)^d	CD ₂ Cl ₂	–80	5.19	4.14	2.77	3.19	1.46	118.2	78.4	44.8
9c(AIRF₄)^d	CD ₂ Cl ₂	–80	5.16	4.08	2.77	3.16	1.46	118.2	78.1	44.9
9c(OTf)	THF- <i>d</i> ₈	–80	5.42	4.76	2.82	3.41	1.50	119.7	82.5	44.9
9c(BF₄)	THF- <i>d</i> ₈	–80	5.43	4.76	2.82	3.42	1.46	119.8	82.7	44.8
9c(PF₆)	THF- <i>d</i> ₈	–80	5.41	4.53	2.85	3.45	1.52	119.8	81.5	45.0
9c(AIRF₄)	THF- <i>d</i> ₈	–80	5.43	4.39	2.91	3.51	1.61	120.0	80.6	45.4
10c(OTf)	THF- <i>d</i> ₈	–80	5.18	4.22	2.90	3.06	1.44	117.2	76.0	45.1
10c(BF₄)	THF- <i>d</i> ₈	–80	5.19	4.17	2.88	3.05	1.43	117.4	75.9	45.2
10c(PF₆)	THF- <i>d</i> ₈	–80	5.23	4.09	2.95	3.07	1.49	117.8	75.6	45.5
10c(AIRF₄)	THF- <i>d</i> ₈	–80	5.21	4.07	2.97	3.08	1.51	117.7	75.4	45.6
11c(BF₄)	CD ₂ Cl ₂	–80	5.14	4.39	3.05br	3.22	1.65br	117.5br	≈78br	br
11c(PF₆)	CD ₂ Cl ₂	–80	5.24	4.46	3.36br	3.29	1.89br	118.5	79.6	54.2
11c(AIRF₄)	CD ₂ Cl ₂	–80	5.25	4.45	3.45br	3.28	1.94br	118.6	≈79.5br	br

	solvent	T, °C	C[N(C ₆ H ₃ -2,6- ⁱ Pr ₂)CH] ₂			
			$\delta(\text{H})$			
			phenyl	NCH	CHMe ₂	CHMe ₂
6c	CD ₂ Cl ₂	25	7.46, 7.30deg	7.19	3.11, 2.83	1.37, 1.32, 1.17, 1.08
6c	THF- <i>d</i> ₈	25	7.40, 7.28deg	7.44	3.23, 2.95	1.36, 1.31, 1.17, 1.07
7c^b	CD ₂ Cl ₂	25	7.41, 7.25deg	7.16	3.13, 2.87	1.32, 1.22, 1.19, 1.06
7c^c	THF- <i>d</i> ₈	25	7.35, 7.23deg	7.39	3.21, 2.93	1.32, 1.23, 1.19, 1.07
8c	CD ₂ Cl ₂	–80	7.49, 7.31deg	7.24	2.77, 2.48	1.28, 1.25, 1.12, 1.02
8c	THF- <i>d</i> ₈	–80	7.52, 7.43deg	7.87	2.93, 2.66	1.38, 1.31, 1.19, 1.10
9c(BF₄)^d	CD ₂ Cl ₂	–80	7.50, 7.32deg	7.28	2.84, 2.50	1.29, 1.21, 1.15, 1.07
9c(PF₆)^d	CD ₂ Cl ₂	–80	7.50, 7.32deg	7.28	2.84, 2.51	1.29, 1.21, 1.15, 1.07
9c(AIRF₄)^d	CD ₂ Cl ₂	–80	7.48, 7.32deg	7.27	2.84, 2.51	1.28, 1.21, 1.15, 1.07
9c(OTf)	THF- <i>d</i> ₈	–80	7.52, 7.43deg	7.87	2.93, 2.66	1.38, 1.31, 1.19, 1.10
9c(BF₄)	THF- <i>d</i> ₈	–80	7.57, 7.48deg	7.90	2.97, 2.64	1.39, 1.31, 1.21, 1.12
9c(PF₆)	THF- <i>d</i> ₈	–80	7.58, 7.49deg	7.88	2.97, 2.67	1.40, 1.32, 1.22, 1.13
9c(AIRF₄)	THF- <i>d</i> ₈	–80	7.58, 7.50deg	7.93	2.96, 2.65	1.40, 1.32, 1.23, 1.13
10c(OTf)	THF- <i>d</i> ₈	–80	7.55, 7.44deg	7.89	2.90, 2.65	1.36deg, 1.23, 1.13
10c(BF₄)	THF- <i>d</i> ₈	–80	7.53, 7.43deg	7.86	2.87, 2.63	1.34deg, 1.20, 1.11
10c(PF₆)	THF- <i>d</i> ₈	–80	7.55, 7.43deg	7.88	2.83, 2.61	1.34deg, 1.21, 1.11
10c(AIRF₄)	THF- <i>d</i> ₈	–80	7.54, 7.44deg	7.91	2.84, 2.61	1.34deg, 1.21, 1.12
11c(BF₄)	CD ₂ Cl ₂	–80	7.50, 7.32deg	7.31	2.61, 2.44	1.27deg, 1.16, 1.07
11c(PF₆)	CD ₂ Cl ₂	–80	7.51, 7.32deg	7.33	2.58, 2.41	1.29, 1.27, 1.17, 1.06
11c(AIRF₄)	CD ₂ Cl ₂	–80	7.51, 7.33deg	7.32	2.59, 2.41	1.29, 1.27, 1.17, 1.06

	solvent	T, °C	PdC	$\delta(\text{C})$						
				phenyl			NCH	CHMe ₂	CHMe ₂	
				ortho	ipso	para				meta
6c	CD ₂ Cl ₂	25	186.2	146.7, 146.5	136.4	130.1	124.2, 124.1	124.7	28.9, 28.8	26.6, 25.8, 23.0, 22.9
6c	THF- <i>d</i> ₈	25	187.2	147.2, 147.0	137.3	130.2	124.3, 124.2	125.4	29.3, 29.2	26.5, 25.9, 23.2, 23.0
7c^b	CD ₂ Cl ₂	25	194.7	146.9, 146.2	137.1	129.6	124.0, 123.9	124.0	28.9, 28.8	26.5, 25.6, 22.9, 22.6
7c^c	THF- <i>d</i> ₈	25	195.2	147.1, 146.5	137.8	129.8	124.1, 124.1	124.6	29.3, 29.1	26.4, 25.6, 23.2, 22.9
8c	CD ₂ Cl ₂	–80	180.4	145.1, 145.0	134.3	129.7	123.7, 123.6	124.4	28.2, 28.1	26.0, 25.1, 22.0, 21.8
8c	THF- <i>d</i> ₈	–80	181.9	146.4deg	136.3	130.9	124.8deg	126.4	29.5deg	26.5, **, 22.8deg
9c(BF₄)^d	CD ₂ Cl ₂	–80	177.7	144.7, 144.6	134.1	130.1	124.0, 123.9	124.3	28.4, 28.1	24.7, 24.5, 22.6, 22.4
9c(PF₆)^d	CD ₂ Cl ₂	–80	177.7	144.7, 144.6	134.1	130.1	124.0, 123.9	124.3	28.4, 28.2	24.7, 24.5, 22.6, 22.4
9c(AIRF₄)^d	CD ₂ Cl ₂	–80	177.7	144.7, 144.6	134.1	130.1	124.0, 123.9	124.3	28.4, 28.2	24.7, 24.4, 22.5, 22.3
9c(OTf)	THF- <i>d</i> ₈	–80	179.8	146.4deg	136.3	130.9	124.8deg	126.4	29.5deg	26.0, **, 22.8deg
9c(BF₄)	THF- <i>d</i> ₈	–80	179.9	146.1deg	136.2	131.1	125.1, 125.0	126.2	29.7, 29.5	25.9, 25.4, 23.1, 23.0
9c(PF₆)	THF- <i>d</i> ₈	–80	179.6	146.1, 146.1	136.1	131.1	125.1, 125.0	126.2	29.7, 29.5	25.9, 25.4, 23.1, 23.0
9c(AIRF₄)	THF- <i>d</i> ₈	–80	179.3	146.2, 146.2	136.1	131.2	125.2, 125.1	126.3	29.7, 29.5	25.9, 25.4, 22.9, 22.9
10c(OTf)	THF- <i>d</i> ₈	–80	182.6	146.6, 146.4	136.1	130.9	124.8deg	126.5	29.4deg	26.5, 25.7, 23.1, 23.0
10c(BF₄)	THF- <i>d</i> ₈	–80	182.5	146.7, 146.5	136.2	130.8	124.8deg	126.5	29.4deg	26.5, 25.7, 23.1, 22.9
10c(PF₆)	THF- <i>d</i> ₈	–80	182.3	146.5, 146.3	136.1	131.0	124.9deg	126.4	29.5deg	26.4, 25.6, 23.1, 22.9
10c(AIRF₄)	THF- <i>d</i> ₈	–80	182.4	146.6, 146.4	136.1	130.9	124.9, 123.8	126.5	29.5deg	26.4, 25.6, 23.0, 22.8
11c(BF₄)	CD ₂ Cl ₂	–80	176.7	145.1, 144.7	133.7	130.2	124.1, 123.9	124.4	28.3, 28.2	25.9, 24.8, 22.7, 22.3
11c(PF₆)	CD ₂ Cl ₂	–80	176.7	145.0, 144.6	133.5	130.3	124.2, 124.0	124.8	28.4, 28.3	26.1, 24.9, 22.7, 22.2
11c(AIRF₄)	CD ₂ Cl ₂	–80	176.5	145.0, 144.6	133.5	130.4	124.2, 124.1	124.8	28.4, 28.3	26.1, 24.9, 22.6, 22.2

^a br = broad. deg = degenerate. *** = overlapped. ^bPdCH₃: $\delta(\text{H})$ –0.37, $\delta(\text{C})$ –18.2. ^cPdCH₃: $\delta(\text{H})$ –0.34, $\delta(\text{C})$ –17.5. ^dTHF ligand: $\delta(\text{H})$ 3.16, 1.62; $\delta(\text{C})$ 74.7, 25.5.

Table 4. Correlation of the Isolated Complexes and the Observed ^1H and ^{13}C NMR Spectra of Tables 2, 3, S2, and S3 and Figures 2, 3, S2, and S3^a

the isolated complexes furnish in CD_2Cl_2 solution at -80°C the NMR signals of ...
8a–d 9a,c(Y) (Y = BF_4 , PF_6 , AIR^{F_4}) 12a,c 11a,c(PF₆) , 13a,c 11a,c(AIR^F₄) , 14a,c	8a–d 9a,c(Y) (Y = BF_4 , PF_6 , AIR^{F_4}) 12a,c in equilibrium with 11a,c(BF₄) 11a,c(PF₆) 11a,c(AIR^F₄)
the isolated complexes furnish in THF- <i>d</i> ₈ solution at -80°C the NMR signals of ...
8a–d 9a,c(BF₄) , 11a,c(BF₄) , 12a,c 9a,c(PF₆) , 11a,c(PF₆) , 13a,c 9a,c(AIR^F₄) , 11a,c(AIR^F₄) , 14a,c	8a–d and 9a–d(OTf) 9a,c(BF₄) 9a,c(PF₆) 9a,c(AIR^F₄)

^a **6a–d** and **7a–d** are unaltered in both CD_2Cl_2 and THF-*d*₈ solutions at -80°C . For complexes **8–14** in particular in THF solution, in the presence of moisture additional signals of the water-solvates **10a–d(Y)** (Y = OTf, BF_4 , PF_6 , AIR^{F_4}) may be observed.

in the solvent (the problem is more evident for the $\text{C}(\text{N}(\text{tBu})\text{CH})_2$ complexes than for the $\text{C}(\text{N}(\text{Ar})\text{CH})_2$ derivatives).²⁷ Deliberate addition of a small quantity of H_2O (or D_2O) to THF solutions of **8a–d** led to complete extinction of the signals of both the undissociated triflates **8a–d** and the THF-solvates **9a–d(OTf)** and the exclusive observation of the ionic water complexes **10a–d(OTf)** as similarly rigid compounds at -80°C (eq 5b, Tables 2, 3, S2, and S3). The displacement of the OTf ligand from Pd(II) by water has precedent.^{28c,f} It can be attributed to the equilibrium of eq 5a that the THF ligand in **9a–d(OTf)** is also readily displaced by water with quantitative formation of **10a–d(OTf)**, despite the competition of the large excess of solvent THF. Thus, water turns out to be a distinctly stronger donor ligand to Pd(II) than either OTf or THF. Various Pd(II)– OH_2 complexes have been isolated and structurally characterized before,²⁸ and some (π -allyl)Pd– H_2O complexes have also been studied.²⁹ **10c(OTf)** is closely related to the very recently isolated nickel complex $[(\eta^3\text{-C}_3\text{H}_5)\text{Ni}\{\text{C}(\text{N}(\text{C}_6\text{H}_3\text{-}2,6\text{-}^i\text{Pr}_2)\text{CH})_2\}(\text{OH}_2)]\text{BARF}$, having low thermal stability.^{11b}

At 25°C the THF-*d*₈ solutions of **8a–d** furnish merely single sets of ^1H and ^{13}C NMR signals, indicating that the equilibrium (eq 5a) between the proper **8a–d** and the THF-solvates **9a–d(OTf)** and, if applicable, the water adducts **10a–d(OTf)** is now so rapid that averaged spectra are observed. Nevertheless, the spectra are still in agreement with an asymmetric π -allyl group and rotating NHC ligand about the Pd–C bond. In detail, for **8a,b** the allyl signals are sharp and the signals of the $\text{C}(\text{N}(\text{tBu})\text{CH})_2$ ligand, which are split at -80°C , are coalesced at 25°C due to the rotation of the ligand. For **8c** the ^1H NMR

signals of H2, H3s, and H3a have remained sharp, but those of H1s and H1a (trans to OTf or THF) are broadened, revealing an incipient selective π - σ -allyl isomerization.^{24,26} Concomitant herewith, the aforementioned split $\text{C}_6\text{H}_3\text{-}2,6\text{-}^i\text{Pr}_2$ signals are now either broadened or already coalesced, indicating local C_{2v} symmetry of the NHC ligand. (The signals correspond to those of the free C_{2v} -symmetrical $\text{C}(\text{N}(\text{C}_6\text{H}_3\text{-}2,6\text{-}^i\text{Pr}_2)\text{CH})_2$, for which diastereotopy of the Me groups rules out rotation about the N–Ar bonds.) In contrast, for the methallyl derivative **8d** the THF-*d*₈ spectra are nicely resolved at ambient temperature (Table S3), as if there were just a single C_1 symmetrical complex with a rigidly bound π -allyl group and a rotating $\text{C}(\text{N}(\text{Ar})\text{CH})_2$ ligand, itself having nonrotating $\text{C}_6\text{H}_3\text{-}2,6\text{-}^i\text{Pr}_2$ substituents, although in fact a rapid exchange occurs according to eq 5a. The reactions of eq 5a must therefore proceed kinetically with retention of the C_1 symmetry.

To summarize the chemical properties that have emerged from the NMR studies, the chlorides **6a–d** and, of course, the methyl complexes **7a–d** do not dissociate in CH_2Cl_2 or THF between -80 and 25°C . In contrast, while the triflates **8a–d** are undissociated in CH_2Cl_2 at -80°C , they partially dissociate in THF with formation of the ionic THF-solvates **9a–d(OTf)**, and this dissociation/solvation occurs more readily for the $\text{C}(\text{N}(\text{Ar})\text{CH})_2$ than for the $\text{C}(\text{N}(\text{tBu})\text{CH})_2$ -containing complexes (there is no obvious effect of 2-Me substitution at the allyl group). Both complexes **8a–d** and **9a–d(OTf)** react quantitatively with water to give the water adducts **10a–d(OTf)**. Aquation of **8a–d** occurs more readily for the $\text{C}(\text{N}(\text{tBu})\text{CH})_2$ than for the $\text{C}(\text{N}(\text{Ar})\text{CH})_2$ derivatives and more readily in THF than in CH_2Cl_2 solution. While the neutral **8a–d** appear to undergo allyl isomerization processes in CH_2Cl_2 at ambient temperature, these processes are reduced in THF solution, where however **8a–d** and the cationic THF-solvates **9a–d(OTf)** are in a rapid equilibrium. With π - σ -allyl isomerization being insignificant, the exchange according to eq 5a occurs with retention of the C_1 symmetry and, hence, the NMR spectra of **8d** are deceptively in agreement with the presence of a single C_1 symmetrical species.

Finally, we come to the chemical shifts of the allyl ^1H and ^{13}C NMR signals of the neutral (π -allyl)Pd(NHC)X complexes **6a–d** to **8a–d** in their rigid structures in CD_2Cl_2 solution (**6a–d** and **7a–d** at 25°C and **8a–d** at -80°C). The NMR shift data of the methallyl complexes are very similar to those of the parent allyl complexes. The correlation of H1s and H1a with C_1 and of H3s and H3a with C_3 has been verified by ^{13}C – ^1H 2D NMR. For **8a–d**, having the weakest donor X = OTf of the sets **6a–d**, **7a–d**, and **8a–d**, the geminal syn and anti allyl protons H3s and H3a and also C_3 (trans to NHC) resonate at relatively low

(27) A similar behavior was observed with cationic Ni–diimine complexes where attempts to isolate the diethyl etherate complexes led to contamination by the corresponding aquo complexes. Svejda, S. A.; Johnson, L. K.; Brookhart, M. *J. Am. Chem. Soc.* **1999**, *121*, 10634.

(28) Isolated Pd(II)– H_2O complexes: (a) Leoni, P.; Sommovigo, M.; Pasquali, M.; Midollini, S.; Braga, D.; Sabatino, P. *Organometallics* **1991**, *10*, 1038. (b) Castan, P.; Jaud, J.; Wimmer, S.; Wimmer, F. L. *J. Chem. Soc., Dalton Trans.* **1991**, 1155. (c) Stang, P. J.; Cao, D. H.; Poulter, G. T.; Arif, A. M. *Organometallics* **1995**, *14*, 1110. (d) Benetollo, F.; Bertani, R.; Bombieri, G.; Toniolo, L. *Inorg. Chim. Acta* **1995**, *233*, 5. (e) Ref 8a. (f) Vicente, J.; Arcas, A.; Bautista, D.; Jones, P. G. *Organometallics* **1997**, *16*, 2127. (g) Vicente, J.; Arcas, A.; Blasco, M.-A.; Lozano, J.; Ramírez de Arellano, M. C. *Organometallics* **1998**, *17*, 5374. (h) Ruiz, J.; Florenciano, F.; Vicente, C.; Ramírez de Arellano, M. C.; López, G. *Inorg. Chem. Commun.* **2000**, *3*, 73. (i) Nama, D.; Schott, D.; Pregosin, P. S.; Veiros, L. F.; Calhorda, M. J. *Organometallics* **2006**, *25*, 4596.

(29) (a) Satsko, N. G.; Belov, A. P.; Moiseev, I. I.; Syrkin, Y. K. *Izv. Akad. Nauk SSSR, Ser. Khim.* **1971**, 2591. (b) Katsman, L. A.; Vargaftik, M. N.; Syrkin, Y. K. *Izv. Akad. Nauk SSSR, Ser. Khim.* **1972**, 1424. (c) Katsman, L. A.; Vargaftik, M. N.; Syrkin, Y. K. *Izv. Akad. Nauk SSSR, Ser. Khim.* **1974**, 299. (d) Katsman, L. A.; Vargaftik, M. N.; Syrkin, Y. K. *Izv. Akad. Nauk SSSR, Ser. Khim.* **1974**, 559. (e) Belov, A. P.; Chubriev, Z. R.; Moiseev, I. I.; Syrkin, Y. K. *Izv. Akad. Nauk SSSR, Ser. Khim.* **1974**, 733.

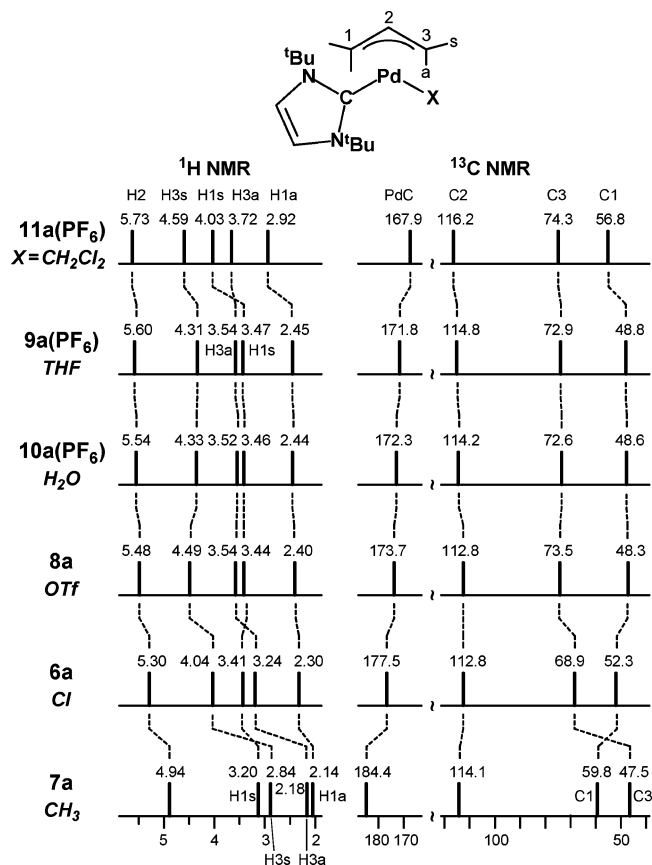


Figure 2. Schematic presentation of the ^1H and ^{13}C NMR resonances of the allyl group and of the ^{13}C resonance of PdC of the NHC ligand for the neutral or cationic $(\eta^3\text{-C}_3\text{H}_5)\text{Pd}\{\text{C}(\text{N}(\text{tBu})\text{-CH}_2)_2\}\text{X}$ complexes **6a**, **7a**, **8a**, **9a**(PF₆), **10a**(PF₆), and **11a**(PF₆) as solutions in CD₂Cl₂. Data from Table 2.

field and H1s, H1a, and C1 (trans to OTf) at higher field, as this is schematically depicted in the lower three traces of Figures 2 and 3 (also Figures S2 and S3). The large chemical shift distinction of the nuclei of the two allyl methylene termini seems in agreement with a reduced electron delocalization and thus polarization of the π -allyl group, so as to display partial carbanionic character at the C1 methylene group and partial olefinic character at the C3 methylene group. In addition to other couplings, there is a small but distinct coupling of about 1 Hz between the “carbanionic” H1s and H1a, but no visible coupling between the “olefinic” H3s and H3a, as part of the characteristics of the signals.

With increasing donor strength of X in the series OTf < Cl < Me, the meso proton H2 and the signals H3s, H3a, and C3 of the methylene group trans to a given NHC ligand experience upfield shifts, to the extent that for the methyl complexes **7a–d** H3s resonates upfield from H1s, H3a approaches H1a (for **7b** H3a has even surpassed H1a), and C3 is shifted upfield from C1. Thus, since the Me group in the PdMe complexes **7a–d** is more strongly electron donating than the NHC ligand, C1, H1s, and H1a (now formally “olefinic”) on one side and C3, H3s, and H3a (now formally “carbanionic”) on the other side have switched their electronic characteristics, which is also indicated in such a detail as the occurrence of geminal coupling between H3s and H3a (and no longer between H1s and H1a).

It follows that in the neutral complexes $(\pi\text{-allyl})\text{M}(\text{L})\text{X}$ (M = Ni, Pd, Pt; L = phosphine or NHC) such as **6–8** it is the relative strength of the (usually weak) anionic donor X that mainly determines the bonding characteristics and chemical shifts of the allyl group, rather than the frequently invoked “trans

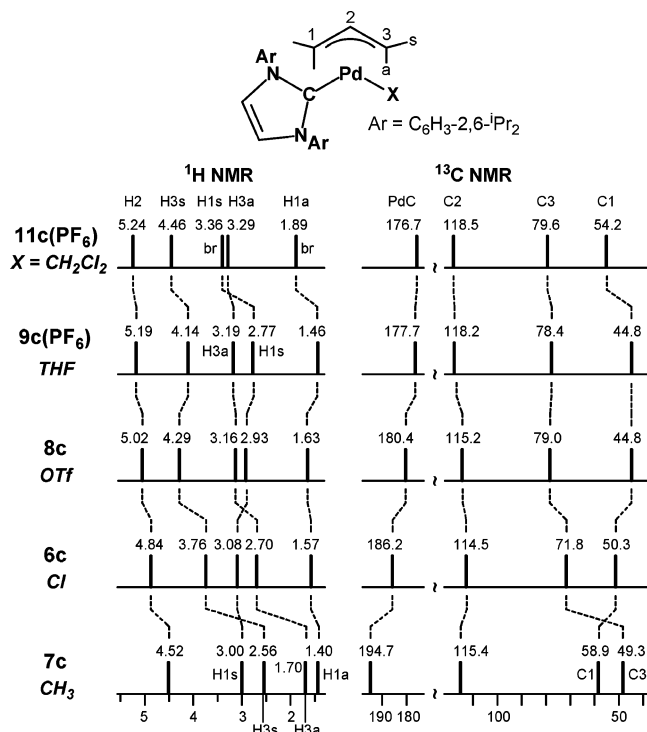


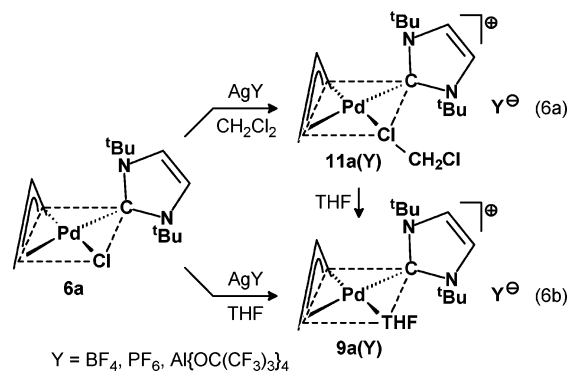
Figure 3. Schematic presentation of the ^1H and ^{13}C NMR resonances of the allyl group and of the ^{13}C resonance of PdC of the NHC ligand for the neutral or cationic $(\eta^3\text{-C}_3\text{H}_5)\text{Pd}\{\text{C}(\text{N}(\text{C}_6\text{H}_3\text{-2,6-}i\text{Pr}_2)\text{CH}_2)_2\}\text{X}$ complexes **6c**, **7c**, **8c**, **9c**(PF₆), and **11c**(PF₆) as solutions in CD₂Cl₂. Data from Table 3.

influence” of the neutral donor ligand L.³⁰ Clearly, in $(\pi\text{-allyl})\text{M}(\text{L})\text{X}$ complexes the chemical shifts of H3s, H3a, and C3 (trans to L) are governed by the cis-positioned X, since X sets the degree of carbanionic character at the trans C1, and hence—by adjusting the electron (de)localization within the allyl group—it rules also the “olefinic” character at C3. We have pointed out this fact previously and have ascribed it to a “communicative effect” within the allyl group.²⁴ We will see at the end of this paper that a special case arises for ionic $[(\pi\text{-C}_3\text{H}_5)\text{Pd}(\text{NHC})(\text{CH}_2\text{-Cl}_2)]^+\text{Y}^-$ complexes with the very poorly donating CH₂Cl₂ ligand.

The chemical shifts of the ionic **9a–d**(OTf) and **10a–d**(OTf) as part of the comprehensive THF-solvates **9a–d**(Y) and water-solvates **10a–d**(Y) (Y = OTf, BF₄, PF₆, AIR^F₄) will be discussed later in this work. Since we observed no particular advantage of the methallyl derivatives over the parent allyl complexes, the following reactions have been carried out only with the parent allyl complexes, that is, for the ligand combinations C₃H₅/C(N^tBu)CH₂ (**a**) and C₃H₅/C(N(C₆H₃-2,6-*i*Pr₂)CH₂) (**c**).

$[(\eta^3\text{-C}_3\text{H}_5)\text{Pd}(\text{NHC})(\text{S})]\text{Y}$ (S = Solvate) (**9a,c**(Y)–**11a,c**(Y)) and $(\eta^3\text{-C}_3\text{H}_5)\text{Pd}(\text{NHC})\text{Y}$ (Y = BF₄, PF₆, AIR^F₄) (**12–14**). When a solution of the C(N^tBu)CH₂-containing **6a** is reacted with 1 equiv of AgBF₄ in CH₂Cl₂ or diethyl ether (20 °C), the corresponding amount of AgCl precipitates. We assume that the intense yellow dichloromethane solution contains the ionic CH₂Cl₂-solvate complex **11a**(BF₄) (eq 6a), which due to its high solubility has not been isolated. Addition of pentane results in the separation of two phases, whereas

(30) Silva, L. C.; Gomes, P. T.; Veiros, L. F.; Pascu, S. I.; Duarte, M. T.; Namorado, S.; Ascenso, J. R.; Dias, A. R. *Organometallics* **2006**, *25*, 4391, and references therein.



evaporation of the solvent at $-30\text{ }^{\circ}\text{C}$ affords the solvent-free **12a** (see below). The diethyl ether solution is light yellow, and upon cooling to $-78\text{ }^{\circ}\text{C}$ only a few microcrystals of a presumed diethyl ether-solvate precipitate. However, addition of THF to one of the above solutions or running the reaction in THF affords a similarly light yellow solution from which the THF adduct **9a**(BF₄) crystallizes nicely at $-40\text{ }^{\circ}\text{C}$ (eq 6b). Crystalline **9a**(BF₄) is stable at ambient temperature, and it seems worth noting that the coordinated THF is not volatile at ambient temperature in high vacuum for several days (in contrast to the CH₂Cl₂ or Et₂O ligands, as in **11a**(BF₄)).

The molecular structure of **9a**(BF₄) is shown in Figure 4, and details of the structure analysis are given in Table S1. The crystal is made up of separate [(η^3 -C₃H₅)Pd{C(N(^tBu)CH)₂-(THF)}] cations and BF₄ anions. In the cation the allyl group is disordered over two positions (63:37), of which only one is shown. The plane of the NHC ligand is perpendicular to the Pd coordination plane, defined by Pd, the terminal carbon atoms of the allyl ligand, and the C and O donor atoms of the NHC and THF ligands, as would be expected for backbonding from the filled d_{xy} orbital lying in the coordination plane into the vacant p at the sp² carbene carbon. In contrast, the THF ligand adopts a more coplanar position to the coordination plane, with what appears to be some overlap of the formally noncoordinating lone electron pair at oxygen with the vacant metal p_z orbital. While the bond distances in the cation appear quite normal (e.g., Pd1–C4 = 2.064(2) Å and Pd1–O1 = 2.185(1) Å), the angle between the NHC ligand and the vicinal carbon of the allyl group, C1–Pd1–C4 = 94.62(8)°, is relatively small, and that between the NHC ligand and the THF ligand, C4–Pd1–O1 = 99.57(6)°, relatively large (cf. the corresponding angles in the BF₄ adduct **12a**), indicating some steric interaction between the NHC and THF ligands. There are no close contacts between the BF₄ anion and the cation, ruling out a specific cation–anion interaction.

Initial attempts to synthesize the PF₆ salts of the cations **9a** and **11a** by reaction of **6a** with commercial AgPF₆ failed, presumably due to the presence of adventitious water in the reagent. These reactions resulted mainly in protonation of the C(N(^tBu)CH)₂ ligand to give the imidazolium salt (see also below) and in partial hydrolysis of PF₆[−] to form difluorophosphate, PO₂F₂[−], for which related reactions were described in the Introduction. Therefore, we have recrystallized the commercial AgPF₆ from Et₂O and, by adding benzene, have also prepared [Ag(C₆H₆)₂]PF₆.

Reaction of **6a** with [Ag(C₆H₆)₂]PF₆ in CH₂Cl₂ gave an intense yellow solution of the CH₂Cl₂-solvate **11a**(PF₆) with the PF₆ counterion (eq 6a). The complex did not crystallize from CH₂Cl₂ solution (similar to **11a**(BF₄)), and addition of a small amount of pentane caused the separation of two phases. However, we have been able to isolate crude yellow **11a**(PF₆)

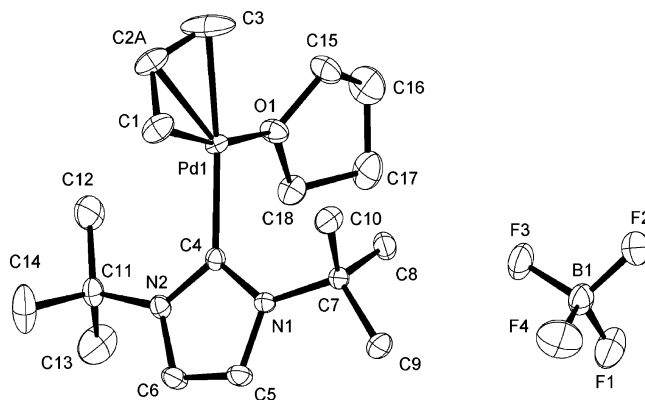
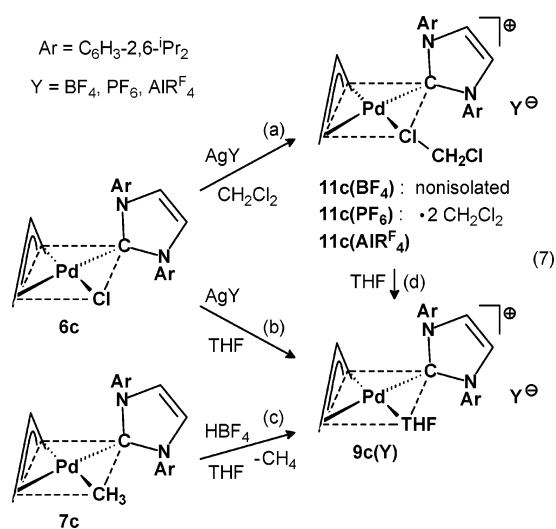


Figure 4. Molecular structure of **9a**(BF₄) in the crystal. Selected bond distances (Å), angles (deg), and interplanar angles (deg): Pd1–C1 = 2.078(2), Pd1–C2A = 2.132(3), Pd1–C3 = 2.194(3), C1–C2A = 1.439(4), C2A–C3 = 1.286(5), Pd1–C4 = 2.064(2), Pd1–O1 = 2.185(1); C1–Pd1–C3 = 68.1(1), C1–Pd1–C4 = 94.62(8), C3–Pd1–O1 = 97.91(9), C4–Pd1–O1 = 99.57(6); C1, C3, Pd1, C4, O1/C4, N1, N2 = 91(1), C1, C3, Pd1, C4, O1/O1, C15, C18 = 29(1).

by evaporation of the solvent at $-35\text{ }^{\circ}\text{C}$. In **11a**(PF₆) the coordinated CH₂Cl₂ is partially volatile at ambient temperature in a vacuum, giving rise to **13a**, as will be shown below. Addition of diethyl ether to the reaction solution allowed the isolation of a pale yellow etherate, having similar properties to **11a**(PF₆), so that it was not studied further. Conducting the reaction in THF led to the isolation of the off-white THF-solvate **9a**(PF₆) (eq 6b), which again is stable under vacuum at ambient temperature.

We have also reacted **6a** with [Ag(CH₂Cl₂)]AIR^F₄ (R^F = OC(CF₃)₃)^{31a} in CH₂Cl₂ to obtain the CH₂Cl₂-solvate **11a**(AIR^F₄) as the AIR^F₄ salt (a precursor to **14a**) (eq 6a). Performing a similar reaction in the presence of THF afforded the THF-solvate **9a**(AIR^F₄) (eq 6b).

In a similar way, the C(N(C₆H₃-2,6-ⁱPr₂)CH)₂-containing **6c** was reacted with AgBF₄ in THF to afford off-white crystals of the ionic THF-solvate complex **9c**(BF₄) (eq 7b). Further access



to **9c**(BF₄) is given by the protolysis of the PdMe complex **7c** with HBF₄ in THF (eq 7c). The isolated **9c**(BF₄) is stable at ambient temperature under vacuum for at least several hours. We did not attempt to isolate the CH₂Cl₂-solvate **11c**(BF₄) (eq

(31) (a) Krossing, I. *Chem.—Eur. J.* **2001**, *7*, 490. (b) Krossing, I.; Raabe, I. *Angew. Chem.* **2004**, *116*, 2116; *Angew. Chem., Int. Ed.* **2004**, *43*, 2066.

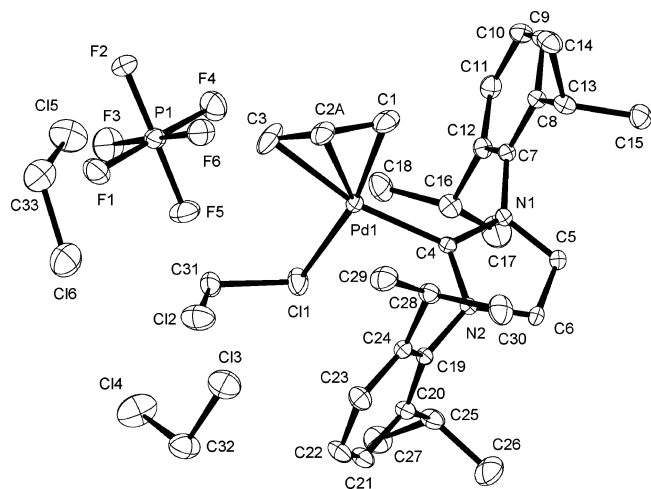


Figure 5. Molecular structure of **11c(PF₆)** in the crystal. For data of the structure analysis, see Table S1. Selected bond distances (Å), angles (deg), and interplanar angle (deg): Pd1–C1 = 2.082(3), Pd1–C2A = 2.154(4), Pd1–C3 = 2.213(4), C1–C2A = 1.342(6), C2A–C3 = 1.401(6), Pd1–C4 = 2.050(3), Pd1–C11 = 2.429(1), C31–C11 = 1.787(3), C31–Cl2 = 1.753(4); C1–Pd1–C3 = 68.09(15), C1–Pd1–C4 = 96.23(13), C3–Pd1–C11 = 100.4(1), C4–Pd1–C11 = 95.3(1); C1, C3, Pd1, C4, C11/C4, N1, N2 = 117(1).

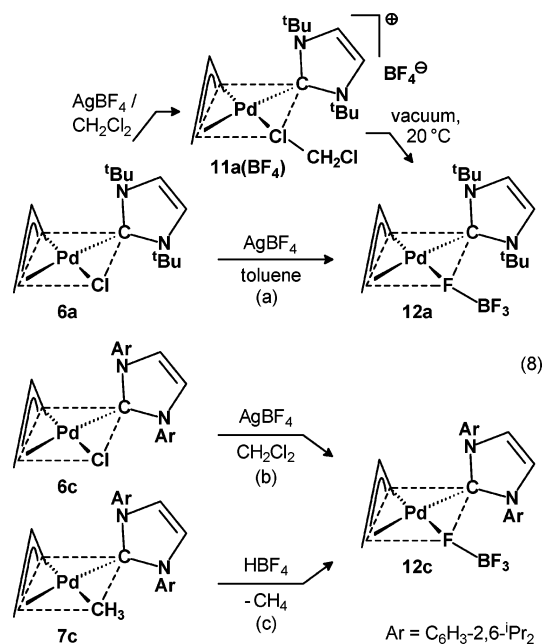
7a) or the corresponding etherate, which we expected to be unstable, as will be seen from a description of the preparation of the solvent-free BF₄ adduct **12c**.

The reaction of **6c** with (commercial) AgPF₆ in CH₂Cl₂ yields, after addition of pentane, pale yellow crystals of the ionic CH₂Cl₂-solvate **11c(PF₆)** (eq 7a). **11c(PF₆)** is stable in the cold (–30 °C), but loses CH₂Cl₂ at ambient temperature under vacuum to give the PF₆ adduct **13c**. Reaction of **6c** with AgPF₆ in THF affords off-white crystals of the stable THF-solvate complex **9c(PF₆)** (eq 7b). The corresponding reaction of **6c** with [Ag(CH₂Cl₂)]AlR^F₄ in CH₂Cl₂ gives **11c(AlR^F₄)** (eq 7a), from which CH₂Cl₂ can be removed to afford the aluminate complex **14c**, as described below in more detail. Treating **11c(AlR^F₄)** with THF affords **9c(AlR^F₄)** (eq 7d).

Complexes **11a,c(Y)** (Y = PF₆, AlR^F₄) appear to be the first isolated Pd complexes in which dichloromethane is bonded to the metal.^{32,33} The result of the crystal structure analysis of **11c(PF₆)** is given in Figure 5, which shows that the compound consists of discrete Pd complex cations and PF₆ anions, together with two additional CH₂Cl₂ solute molecules. The coordination geometry of the Pd center is planar with the terminal methylene groups of the π -allyl ligand, the NHC ligand, and one chlorine atom of a CH₂Cl₂ ligand occupying the coordination sites. The meso carbon atom of the allyl ligand is slightly disordered over two positions (refined occupancy of C2A: 0.72(1)). The complex is best compared to the neutral chloride **6c**.^{21b} Of particular interest is the coordination bond of the CH₂Cl₂ ligand to Pd in **11c(PF₆)**, which at Pd1–C11 = 2.429(1) Å is slightly

longer than Pd–Cl in **6c** (2.370 Å). This has a consequence on the allyl coordination, and the Pd–C bond trans to the CH₂Cl₂ ligand, Pd1–C1 = 2.082(3) Å, is shorter and that trans to the NHC ligand, Pd1–C3 = 2.213(4) Å, is longer than the corresponding bonds in **6c** (2.110 and 2.201 Å). In agreement within some π -electron localization of the allyl ligand the bonds C1–C2A = 1.342(6) Å and C2A–C3 = 1.401(6) Å are quite different in length, similar to the situation observed in **6c** (1.375 and 1.414 Å). The Pd–C distance to the NHC ligand at 2.050(3) Å is as expected (**6c**, 2.040 Å).

For the successful synthesis of solvent-free (η^3 -C₃H₅)Pd–(NHC)(BF₄) complexes, the chlorides **6a,c** have first been reacted with AgBF₄ in CH₂Cl₂. Starting from **6a**, the intermediately formed weak CH₂Cl₂ adduct **11a(BF₄)** readily loses CH₂Cl₂ when drying it at ambient temperature in a vacuum to give the BF₄ adduct **12a** as a powder. Recrystallization of the product from toluene gave yellow crystals, suitable for an X-ray structure determination. It has subsequently been shown that the whole synthesis can be carried out in toluene to afford directly crystalline **12a** (eq 8a). Synthesis of **12a** from the PdMe complex **7a** by protolysis with HBF₄ is not feasible for the reasons described above.



The molecular structure of **12a** is shown in Figure 6. The complex is akin to the chloride **6a**,^{21b} containing the same NHC ligand. It is also closely related to the Ni complexes **1a,b** mentioned in the Introduction. The early literature on BF₄ complexes has been reviewed.^{34a} While the CSD^{33c} currently lists over a hundred crystal structures of transition metal BF₄ complexes, there is only one other structure of a Pd complex with a coordinatively bound BF₄ anion, and this exhibits a nonplanar metal coordination geometry (Pd–F = 2.355(5) Å, μ -F–B = 1.419(9) Å).^{34b} In **12a** the coordination of the Pd(II) center is planar, with the terminal allyl carbon atoms C1 and C3, the NHC carbon atom C4, and one fluorine atom (F1) of the monodentate BF₄ ligand occupying the coordination sites. Although substantially longer than Pd–F bonds of terminal fluorides (typically 2.02–2.09 Å),³⁵ the Pd1–F1 bond length at 2.241(2) Å is markedly shorter and the B1–F1 bond at 1.432(3) Å is longer than in the crystal structure of the other Pd–

(32) The formation of Pd–dichloromethane complexes in solution has been proposed: (a) Kraatz, H.-B.; Milstein, D. *J. Organomet. Chem.* **1995**, *488*, 223. (b) Ankersmit, H. A.; Witte, P. T.; Kooijman, H.; Lakin, M. T.; Spek, A. L.; Goubitz, K.; Vrieze, K.; van Koten, G. *Inorg. Chem.* **1996**, *35*, 6053. (c) Desjardins, S. Y.; Way, A. A.; Murray, M. C.; Adirim, D.; Baird, M. C. *Organometallics* **1998**, *17*, 2382. (d) Foley, S. R.; Stockland, R. A., Jr.; Shen, H.; Jordan, R. F. *J. Am. Chem. Soc.* **2003**, *125*, 4350.

(33) (a) For the molecular structure of [trans-(η^3 -Pr₃P)₂Pt(H)(CH₂Cl₂)]-BARF, see: Butts, M. D.; Scott, B. L.; Kubas, G. J. *J. Am. Chem. Soc.* **1996**, *118*, 11831. (b) At the present time a total of 18 transition metal dichloromethane complexes are listed in the Cambridge Structural Database,^{33c} mostly complexes of Ag (9), Rh (3), Ru (2), and Re (2). (c) Cambridge Structural Database (CSD), version 5.27, update of January 2006.

(34) (a) Beck, W.; Sünkel, K. *Chem. Rev.* **1988**, *88*, 1405. (b) Rheingold, A. L.; Wu, G.; Heck, R. F. *Inorg. Chim. Acta* **1987**, *131*, 147.

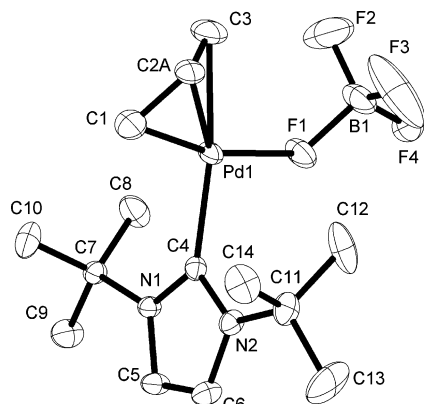
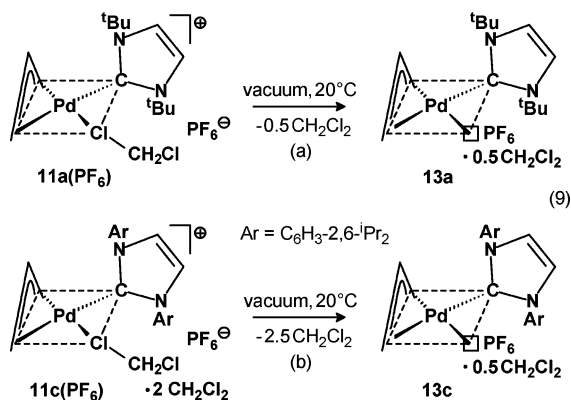


Figure 6. Molecular structure of **12a** in the crystal. For data of the structure analysis, see Table S1. Selected bond distances (Å), angles (deg), and interplanar angle (deg): Pd1–C1 = 2.082(3), Pd1–C2A = 2.125(5), Pd1–C3 = 2.185(3), C1–C2A = 1.408(6), C2A–C3 = 1.369(6), Pd1–C4 = 2.067(2), Pd1–F1 = 2.241(2), B1–F1 = 1.432(3); C1–Pd1–C3 = 68.1(1), C1–Pd1–C4 = 101.0(1), C3–Pd1–F1 = 98.0(1), C4–Pd1–F1 = 92.87(7), Pd1–F1–B1 = 128.0(2); C1,C3,Pd1,C4,F1/C4,N1,N2 = 89(1).

BF₄ complex, indicating a relatively strong coordination of BF₄ to Pd (mean length of the other three B–F bonds: 1.363 Å). Otherwise, the (η^3 -C₃H₅)Pd moiety in **12a** shows the expected short Pd1–C1 bond at 2.082(3) Å (the very same as for the CH₂Cl₂ adduct **11c**(PF₆)) and long Pd1–C3 bond at 2.185(3) Å. The mean plane of the NHC ligand lies approximately orthogonal (89°) to the coordination plane of the metal.

When **6c** is reacted with AgBF₄ in CH₂Cl₂, after removal of AgCl and addition of pentane, the solvent-free pale yellow **12c** crystallizes directly from the solution (eq 8b). In addition, complex **12c** has been obtained by protolysis of **7c** with 1 equiv of HBF₄ in a diethyl ether–CH₂Cl₂ mixture (eq 8c). It seems reasonable to assume that in the solution the CH₂Cl₂-solvate **11c**(BF₄) or the corresponding Et₂O-solvate is present. However, the cationic (π -allyl)Pd(NHC) kernel is obviously highly electrophilic since it associates with the weakly nucleophilic BF₄ anion upon crystallization to form the neutral solvate-free **12c**. The structure of **12c** is presumably similar to that of **12a**.

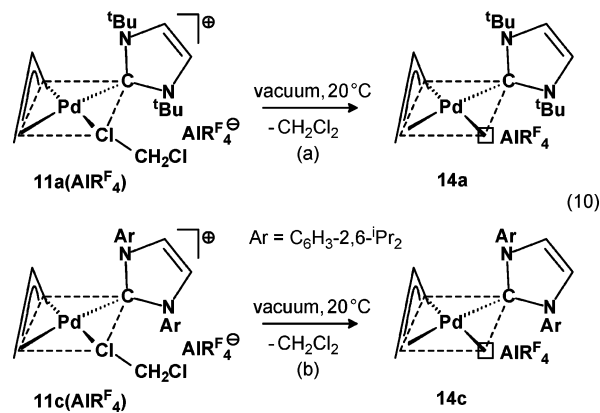
In analogy to **12a,c**, we attempted to synthesize solvate-free (η^3 -C₃H₅)Pd(NHC)Y complexes with the even weaker nucleophiles Y = PF₆ and AIR₄⁺. When the yellow powdery CH₂Cl₂-solvate **11a**(PF₆) and the well-formed pale yellow crystals of **11c**(PF₆) are subjected to a vacuum at ambient temperature for



1 h, the coordinated (and solute) CH₂Cl₂ is largely released to leave **13a,c** (eq 9). According to NMR and elemental analysis, the products persistently retained about 1/2 CH₂Cl₂. The analysis of all the PF₆ salts in this report is made difficult by the possible

hydrolysis of the PF₆ anion by inevitable moisture (see above).³⁶ **13a** is microcrystalline and as yet not suitable for a single-crystal structure determination. In the case of **13c**, the well-shaped crystals of the primary **11c**(PF₆) showed no visible alteration after the drying, so that the CH₂Cl₂ appears to have evaporated without destruction of the lattice, but so far it has not been possible to obtain data useful for an X-ray structure analysis of **13c**. With respect to the structure of **13a,c** we are left to speculate whether the 1/2 CH₂Cl₂ represents a solute molecule in the lattice (cf. **11c**(PF₆)), with the PF₆ anion coordinating via a bridging fluoride at the Pd atom, similar to the BF₄ anion in **12a,c**, or whether the structure is dinuclear with a μ -CH₂Cl₂ ligand, for which there is also precedent.³⁷

When the crystalline CH₂Cl₂-solvates **11a,c**(AIR₄⁺) are subjected to a vacuum at ambient temperature for 2 h, they readily release *all* CH₂Cl₂ to yield the neutral products **14a,c** (eq 10), displaying correct elemental analyses. These complexes



form yellow (**14a**) and pale yellow (**14c**) powders, and it has not been possible to carry out an X-ray single-crystal structure analysis. Thus, so far it is not known whether solids **14a,c** are truly ionic with internally stabilized or T-shaped 14e [(η^3 -C₃H₅)Pd(NHC)]⁺ cations³⁸ or whether the indeed fiercely electrophilic cations associate with the otherwise typically noncoordinating AIR₄⁺^{31b} via some weak Pd– μ -F–C interaction. The fact that for **11a,c**(Y) the release of all the CH₂Cl₂ in the vacuum proceeds much easier with the AIR₄⁺ than with the PF₆[−] counterion may result from the larger size of the anion and a different lattice. Complexes **13a,c** and **14a,c** are insoluble in typically noncoordinating toluene. Dissolution of **13a,c** and **14a,c** in CH₂Cl₂ leads to recovery of **11a,c**(Y) (Y = PF₆, AIR₄⁺).

(35) (a) Grushin, V. V.; Marshall, W. *J. Angew. Chem., Int. Ed.* **2002**, *41*, 4476, and references therein. (b) Yahav, A.; Goldberg, I.; Vialok, A. *J. Am. Chem. Soc.* **2003**, *125*, 13634. (c) Jasim, N. A.; Perutz, R. N.; Whitwood, A. C.; Braun, T.; Izundu, J.; Neumann, B.; Rothfeld, S.; Stammmer, H.-G. *Organometallics* **2004**, *23*, 6140.

(36) F[−] abstraction from PF₆[−] must also be taken into account. (a) Jordan, R. F.; Dasher, W. E.; Echols, S. F. *J. Am. Chem. Soc.* **1986**, *108*, 1718. (b) Bochmann, M.; Wilson, L. M.; Hursthouse, M. B.; Short, R. L. *Organometallics* **1987**, *6*, 2556.

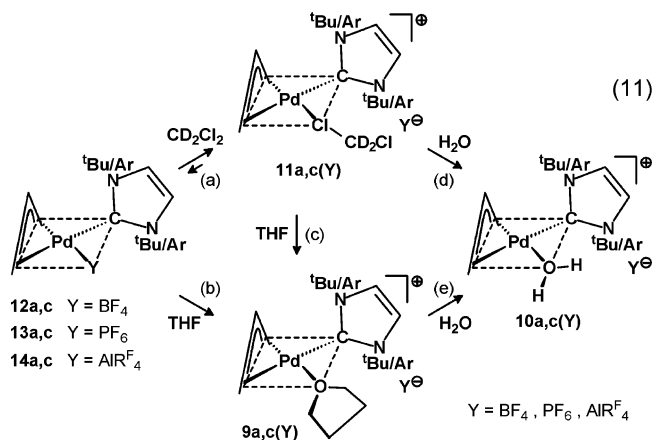
(37) Bown, M.; Waters, J. M. *J. Am. Chem. Soc.* **1990**, *112*, 2442.

(38) Several ionic or neutral, seemingly three-coordinate 14e Ni^{II}- and Pd^{II}-organyl complexes that feature an additional β -H agostic interaction have been described in recent years. (a) [(^tBu₂PC₂H₄P^tBu₂)Ni(C₂H₅)](BF₄); Conroy-Lewis, F. M.; Mole, L.; Redhouse, A. D.; Litster, S. A.; Spencer, J. L. *J. Chem. Soc., Chem. Commun.* **1991**, 1601. (b) (R₃P)Pd(Ar)X (X = Br, I, OTf); Stambuli, J. P.; Bühl, M.; Hartwig, J. F. *J. Am. Chem. Soc.* **2002**, *124*, 9346, ref 19f. (c) [(α -diimine)MR][BAR₄] (M = Ni, Pd; R = Et, Pr); Tempel, D. J.; Johnson, L. K.; Huff, R. L.; White, P. S.; Brookhart, M. *J. Am. Chem. Soc.* **2000**, *122*, 6686. Shultz, L. H.; Tempel, D. J.; Brookhart, M. *J. Am. Chem. Soc.* **2001**, *123*, 11539. Leatherman, M. D.; Svejda, S. A.; Johnson, L. K.; Brookhart, M. *J. Am. Chem. Soc.* **2003**, *125*, 3068. (d) (β -diketiminate)NiR (R = Et, Pr): Kogut, E.; Zeller, A.; Warren, T. H.; Strassner, T. *J. Am. Chem. Soc.* **2004**, *126*, 11984.

The various ionic solvate complexes $[(\eta^3\text{-C}_3\text{H}_5)\text{Pd}(\text{NHC})\text{-}(\text{S})\text{Y}]$ (**9**, **11**) and the neutral solvent-free complexes $(\eta^3\text{-C}_3\text{H}_5)\text{-Pd}(\text{NHC})\text{Y}$ (**12**–**14**) ($\text{Y} = \text{BF}_4, \text{PF}_6, \text{AIR}^{\text{F}_4}$) show in the ESIpos mass spectra (CH_2Cl_2) for the isolated **9a**(**Y**) ($\text{Y} = \text{BF}_4, \text{PF}_6, \text{AIR}^{\text{F}_4}$), **11a**(AIR^{F_4}), **12a**, **13a**, and **14a** uniformly $[(\eta^3\text{-C}_3\text{H}_5)\text{Pd}\{\text{C}(\text{N}(\text{tBu})\text{CH}_2)_2\}]^+$ ($m/e = 327$) and for the likewise isolated **9c**(**Y**) ($\text{Y} = \text{BF}_4, \text{PF}_6, \text{AIR}^{\text{F}_4}$), **11c**(**Y**) ($\text{Y} = \text{PF}_6, \text{AIR}^{\text{F}_4}$), **12c**, **13c**, and **14c** uniformly $[(\eta^3\text{-C}_3\text{H}_5)\text{Pd}\{\text{C}(\text{N}(\text{C}_6\text{H}_3\text{Pr}_2)\text{-CH}_2)_2\}]^+$ ($m/e = 535$) as the largest observable ion, resulting from cleavage of the $\text{BF}_4, \text{PF}_6,$ or AIR^{F_4} anion and (where appropriate) of the solvent ligand. Correspondingly, in the ESI_{neg} mass spectra the signals of the BF_4 (two signals due to the ^{10}B and ^{11}B isotopomers), $\text{PF}_6,$ or AIR^{F_4} ions are found. Thus, the ESI mass spectra are in agreement with the given compositions of the complexes, but they cannot distinguish between the ionic solvates and the neutral solvent-free complexes. All complexes decompose under the conditions of EIMS.

The ^1H and ^{13}C NMR spectra of complexes **9a,c**(**Y**)–**14a,c** ($\text{Y} = \text{BF}_4, \text{PF}_6, \text{AIR}^{\text{F}_4}$) have been recorded in CD_2Cl_2 and $\text{THF-}d_8$ as solvents. Information on the structure of the complexes in solution is best obtained from the low-temperature spectra ($-80\text{ }^\circ\text{C}$), and the respective chemical shifts are listed in Tables 2 and 3, together with the previously discussed data of the corresponding triflate complexes **8a,c** and **9a,c**(**Y**) for $\text{Y} = \text{OTf}$. As for the triflate complexes, the solutions of the $\text{C}(\text{N}(\text{tBu})\text{-CH}_2)_2$ -containing **9a**(**Y**), **11a**(**Y**), **12a**, **13a**, and **14a** are particularly very sensitive to the presence of traces of moisture, thereby giving rise to small but varying amounts of additional water-solvate complexes **10a**(**Y**).²⁷

The NMR spectra of the isolated ionic THF-solvates **9a,c**(**Y**) ($\text{Y} = \text{BF}_4, \text{PF}_6, \text{AIR}^{\text{F}_4}$) at $-80\text{ }^\circ\text{C}$ are fully resolved for CD_2Cl_2 and somewhat less so for $\text{THF-}d_8$. In CD_2Cl_2 the THF ligand remains coordinated (**9a**(**Y**): $\delta(\text{C})$ 75.5 and 25.9, compared with $\delta(\text{C})$ 68.2 and 26.4 for uncoordinated THF), but in $\text{THF-}d_8$ it undergoes slow solvent exchange. The spectra of **9a,c**(**Y**) are also observed when the isolated CH_2Cl_2 -solvates **11a,c**(**Y**) ($\text{Y} = \text{PF}_6, \text{AIR}^{\text{F}_4}$) or the solvate-free **12a,c**–**14a,c** are dissolved in $\text{THF-}d_8$ (see correlation in Table 4), since Pd becomes solvated by $\text{THF-}d_8$ (eqs 11b,c). **9a,c**(**Y**) represents



the only complex in solution, notwithstanding a minor amount of **10a**(**Y**) as an impurity. The ^1H and ^{13}C chemical shifts of **9a**(**Y**) ($\text{Y} = \text{BF}_4, \text{PF}_6$) and **9c**(**Y**) ($\text{Y} = \text{BF}_4, \text{PF}_6, \text{AIR}^{\text{F}_4}$) in CD_2Cl_2 and of **9a,c**(**Y**) ($\text{Y} = \text{OTf}, \text{BF}_4, \text{PF}_6, \text{AIR}^{\text{F}_4}$) in $\text{THF-}d_8$ show only little variance with the different counterions (Tables 2 and 3). Those small variances observed in particular for the allyl H1s/a and H3s/a resonances can be attributed to ion pairing,³⁹ which is not unexpected in solvents of low dielectric

constant. There is, however, a distinct solvent effect for isolated **9a,c**(**Y**) when changing the solvent from CD_2Cl_2 to $\text{THF-}d_8$, resulting in a shift of all ^1H allyl and NHC signals to markedly lower field. As has already been noted for the (nonisolated) THF- solvates **9a,c**(**OTf**) with the triflate counterion, the $-80\text{ }^\circ\text{C}$ spectra of **9a,c**(**Y**) in both solvents support a C_1 symmetrical structure of the complexes, with **9a**(**Y**) having a nonrotating $\text{C}(\text{N}(\text{tBu})\text{CH}_2)_2$ ligand due to the bulkiness of this ligand and **9c**(**Y**) having a rotating $\text{C}(\text{N}(\text{Ar})\text{CH}_2)_2$ ligand with rigid $N\text{-C}_6\text{H}_3\text{-}2,6\text{-iPr}_2$ substituents. In the ambient-temperature $\text{THF-}d_8$ spectra of **9a,c**(**Y**) the allyl resonances remain consistent with a C_1 symmetrical structure, with the NHC signals indicating rotation about the $\text{Pd}=\text{C}$ bonds, but in the CD_2Cl_2 spectra the allyl methylene resonances are so broad that they can hardly be located any more.

The NMR spectra of the isolated ionic CH_2Cl_2 -solvates **11a,c**(**Y**) ($\text{Y} = \text{PF}_6, \text{AIR}^{\text{F}_4}$) must be recorded in CD_2Cl_2 solution, and here the initially coordinated CH_2Cl_2 is exchanged with CD_2Cl_2 . Furthermore, the solutions of the adducts **13a,c** and **14a,c** in CD_2Cl_2 give rise to essentially the same spectra as for the corresponding isolated ionic **11a,c**(**Y**), indicating that **13a,c** and **14a,c** become resolvated in CD_2Cl_2 to give **11a,c**(**Y**) ($\text{Y} = \text{PF}_6, \text{AIR}^{\text{F}_4}$). Similar spectra are observed when **12a,c** are dissolved in CD_2Cl_2 , suggesting that they become fully or partially solvated to form (nonisolated) **11a,c**(BF_4) (eq 11a and Table 4). While for the different counterions $\text{Y} = \text{BF}_4, \text{PF}_6, \text{AIR}^{\text{F}_4}$ the variance of the spectra of **11a**(**Y**) in CD_2Cl_2 is only marginal (Table 2; see, however, H3s), that of **11c**(**Y**) (Table 3) is more pronounced, in particular for the allyl ^1H NMR data of **11c**(BF_4). Again, the differences seem to be due to individual ion pairing, and we assume that the neutral **12c** is in a well-balanced equilibrium with its CH_2Cl_2 -solvate **11c**(BF_4).

A characteristic feature of the $\text{C}(\text{N}(\text{tBu})\text{CH}_2)_2$ -ligated CH_2Cl_2 -solvates (respectively CD_2Cl_2 -solvates) **11a**(**Y**) ($\text{Y} = \text{BF}_4, \text{PF}_6, \text{AIR}^{\text{F}_4}$) with a likewise C_1 symmetrical structure (all allyl protons and carbon atoms are inequivalent) appears to be that the otherwise split signals of the $\text{C}(\text{N}(\text{tBu})\text{CH}_2)_2$ ligand are coalesced at $-80\text{ }^\circ\text{C}$ (Table 2), so that here the ligand rotates at low temperature. The fact is particularly noteworthy, since in the other complexes, including the ionic THF- solvates **9a**(**Y**) described above, the $\text{C}(\text{N}(\text{tBu})\text{CH}_2)_2$ ligand is rigid at the same temperature, and for the neutral chlorides **6a,b** and the PdMe complexes **7a,b** this is true even at ambient temperature. We attribute the low rotational barrier of the $\text{C}(\text{N}(\text{tBu})\text{CH}_2)_2$ ligand to a particularly weak coordination and consequently low steric effect of the vicinal $\kappa^1\text{-Cl-CH}_2\text{Cl}$ ligand, resulting in a situation *as if* there were a free coordination site.

The general structural features of the $\text{C}(\text{N}(\text{Ar})\text{CH}_2)_2$ -ligated CH_2Cl_2 -solvates **11c**(**Y**) ($-80\text{ }^\circ\text{C}$) correspond to those of the THF- solvates **9c**(**Y**); that is, the complexes display C_1 symmetry with a rotating $\text{C}(\text{N}(\text{C}_6\text{H}_3\text{-}2,6\text{-iPr}_2)\text{CH}_2)_2$ ligand having itself nonrotating $N\text{-C}_6\text{H}_3\text{-}2,6\text{-iPr}_2$ substituents, as evidenced by the typical distribution of the allyl and NHC NMR signals (Table 3). However, while all allyl ^1H resonances in **11c**(**Y**) are distinct, slight broadening of H3s and H3a and pronounced broadening of H1s and H1a and also of C3 and C1 can be attributed to incipient selective $\pi\text{-}\sigma$ -allyl isomerizations,^{24,26} which apparently occur for both ends of the allyl group at different rates.

As expected, most allyl ^1H and ^{13}C NMR resonances of **11a,c**(**Y**) lie at lowest field compared to the allyl resonances of the

(39) (a) For recent NMR studies on the degree of ion pairing in Pd complexes, see: Schott, D.; Pregosin, P. S.; Veiros, L. F.; Calhorda, M. J. *Organometallics* **2005**, *24*, 5710, ref. 28i. (b) A detailed NMR investigation of the ion pairing was beyond the scope of this work.

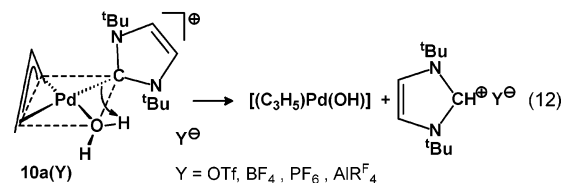
other neutral and cationic complexes ($\eta^3\text{-C}_3\text{H}_5$)Pd{C(N(^tBu)-CH₂)₂}X and ($\eta^3\text{-C}_3\text{H}_5$)Pd{C(N(C₆H₃-2,6-ⁱPr₂)CH₂)₂}X. However, as can be seen from Figures 2 and 3 (exemplified here for X/Y = PF₆), there is an interesting course in the allyl chemical shifts with decreasing donor strength of X. Starting from **7a,c** with X = Me as the strongest donor, in the series **7a,c** → **6a,c** → **8a,c** it is initially H3s, H3a, and C3 trans to the NHC ligand that are significantly shifted downfield, as described in the preceding section of the paper. Continuing in the series **8a,c** → **10a(Y)** → **9a,c(Y)** with the O-donor ligands OTf, H₂O, and THF, only a slight continued downfield shift of most allyl resonances occurs. On changing from the THF-solvates to the CH₂Cl₂-solvates, **9a,c(Y)** → **11a,c(Y)**, it is now, however, principally H1s and H1a (by about 0.5 ppm) and C1 (by 8–10 ppm) of the allyl methylene group trans to the CH₂Cl₂ ligand that are significantly shifted further downfield (and less so H3s, H3a, and C3 trans to NHC). Apparently, H1s, H1a, and C1 strive to align with H3s, H3a, and C3, instead of further divergence. This may arise from the particular weak coordination of the CH₂Cl₂ ligand, allowing the NHC ligand to assume a coordination situation as if it were more directly opposite the allyl group. This feature would agree with the observed low rotational barrier of the C(N(^tBu)CH₂)₂ ligand in **11a(Y)** and would also explain the occurrence of (inequivalent) π - σ -allyl isomerizations^{24,26} at both ends of the allyl group in **11c(Y)**. The CH₂Cl₂-solvates **11a,c(Y)** are thus quite distinct from the other solvate complexes.

It seems appropriate to discuss at this point the features of the nonisolated, likewise ionic water-solvates **10a,c(Y)** (Y = OTf, BF₄, PF₆, AIR^F₄). For the C(N(^tBu)CH₂)₂-ligated **8a**, **9a(Y)**, **11a(Y)**, **12a**, **13a**, and **14a** in THF-*d*₈ solution at -80 °C additional NMR signals were found, which can be attributed to the water-solvates **10a(Y)**. This occurred even when the solvents were dried over NaAlEt₄, which ranks among one of the most effective drying agents, so we assume that the water possibly originated from the glassware surfaces. Deliberate addition of small amounts of water (D₂O in order to minimize solvent signals) at -60 °C to such solutions, including also the C(N(Ar)-CH₂)₂ derivatives, led to quantitative formation of **10a,c(Y)** (eqs 11d,e), so that the spectra of the pure water-solvates have been observed. Hydration was markedly slower in CD₂Cl₂ solution, which may be due to poor mixing of CD₂Cl₂ and water, especially at low temperature. By this method the NMR data of **10a(Y)** in both CD₂Cl₂ (Y ≠ OTf) and THF-*d*₈ (Table 2) and of **10c(Y)** in THF-*d*₈ (Table 3) with the various counterions Y = OTf, BF₄, PF₆, AIR^F₄ have been collected at -80 °C.

As for the THF-solvates **9a,c(Y)**, the NMR spectra of **10a,c(Y)** are in agreement with C₁ symmetrical structures of the complexes with a nonrotating C(N(^tBu)CH₂)₂ ligand (**10a(Y)**) but a rotating C(N(C₆H₃-2,6-ⁱPr₂)CH₂)₂ ligand (**10c(Y)**). It is left open at this time whether the orientation of the water ligand is coplanar with the Pd coordination plane—as for the THF ligand in **9a(BF₄)**—or perpendicular, as in the other Pd(II)-OH₂ complexes, where it is H-bonded to the anions.²⁸ Perusal of the NMR data of **10a,c(Y)** shows for each group of compounds in a given solvent typical ranges of the NMR chemical shifts of the allyl and NHC ligands, but at the same time also distinct variations within each group, in particular for the allyl protons. We again attribute these variations to different degrees of ion pairing that result from the various hydrogen bonds between the coordinated water and the individual anions.²⁸ The reaction of eq 11e suggests that water represents a distinctly stronger donor than THF, perhaps due to Pd-OH...H⁺...Y⁻ formation, and this fact is also reflected in the NMR chemical shifts of the

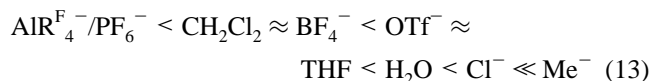
allyl groups, which for the water adducts **10a(Y)** in THF-*d*₈ are markedly at higher field than for the THF-solvates **9a(Y)** (Table 2), although the effect is smaller in CD₂Cl₂ solution (Table 2 and Figure 2).

When the temperature is raised from -80 °C to ambient, the various species in solution (e.g., **9a(Y)** and **10a(Y)**, or **11a(Y)** and **10a(Y)**) equilibrate, so that only one set of signals is observed. Furthermore, a gradual protonation of the C(N(^tBu)-CH₂)₂ ligand to give the imidazolium salt is found, possibly by an intramolecular mechanism (eq 12). Generation of an intermediate Pd(II)-OH₂ adduct such as **10a(PF₆)** may also explain the failure of the synthesis of **9a(PF₆)** and **11a(PF₆)** with commercial AgPF₆ and instead the observed decomposition with formation of the imidazolium salt.



Because of the reasons described above, the isolated complexes **8–14** furnish in solution (THF-*d*₈ or CD₂Cl₂) the NMR spectra of **8a–d**, **9a–d(OTf)**, **9a,c(Y)** (Y = BF₄, PF₆, AIR^F₄), **10a–d(OTf)**, **10a,c(Y)** (Y = BF₄, PF₆, AIR^F₄), and **11a,c(Y)** (Y = BF₄, PF₆, AIR^F₄) (see correlation in Table 4; **6** and **7** remain unaltered in solution). In the observed complexes, besides the allyl group, the NHC ligand also represents a spectator ligand for the electronic situation of the Pd(II) center. As the data of Tables 2 and 3 (Figures 2 and 3) show, the chemical shift δ (PdC) of the NHC donor C atom⁴⁰ coordinated to Pd is smallest for the undoubtedly electron-poorest CH₂Cl₂-solvates **11a,c(Y)**, but it increases in the descending order of the traces in Figures 2 and 3 by $\Delta\delta$ (PdC) = 16–18 ppm to become largest for the electron-rich PdMe complexes **7a–d**. This change of the chemical shift follows that established previously for CO ligands, which show a diminishing shielding of the carbonyl-C atoms with an increasing charging of the metal center and, hence, increasing back-bonding to the CO ligand.⁴¹ Thus, the deshielding of the NHC donor C atom that is observed when going from **11a,c(Y)** to **7a–d** can be taken as unequivocal experimental evidence for an enhanced back-bonding in this series between Pd(II) and the otherwise strongly electron-donating NHC ligand.⁴²

To summarize, for the anions and solvate ligands chemical and NMR spectroscopical evidence supports an increasing donor strength/nucleophilicity toward the $[(\pi\text{-allyl})\text{Pd}(\text{NHC})]^+$ moiety in the series



(40) Regarding uncoordinated NHCs, the resonance of the carbene-C atom of C(N(^tBu)CH₂)₂ is at δ (C) 213.2 (THF-*d*₈)^{45a} and that of C(N(C₆H₃-2,6-ⁱPr₂)CH₂)₂ is at δ (C) 220.2 (C₆D₆)^{45c} thus downfield from the shifts of the Pd(II) complexes.

(41) (a) Bodner, G. M. *Inorg. Chem.* **1975**, *14*, 1932. (b) Kleimann, W.; Pörschke, K.-R.; Wilke, G. *Chem. Ber.* **1985**, *118*, 323.

(42) Although backbonding in M-NHC complexes was initially disregarded, it appears now well-accepted, mainly on the basis of DFT calculations. (a) For a review on this issue, see: Hu, X.; Meyer, K. J. *Organomet. Chem.* **2005**, *690*, 5474. (b) For recent experimental evidence, see: Mercs, L.; Labat, G.; Neels, A.; Ehlers, A.; Albrecht, M. *Organometallics* **2006**, *25*, 5648. Sanderson, M. D.; Kamplain, J. W.; Bielawski, C. W. *J. Am. Chem. Soc.* **2006**, *128*, 16514.

In this series AlR_4^+ and PF_6^- appear as the weakest donors, and from CH_2Cl_2 solution inevitably the ionic CH_2Cl_2 -solvates **11a,c(Y)** ($Y = \text{PF}_6, \text{AlR}_4^+$) separate. **11a,c(Y)** are not isolable for $Y = \text{BF}_4$ and OTf: while **11a,c(BF₄)** are assumed to be present in CH_2Cl_2 solution and separate from such solutions as the solvent-free **12a,c**, in agreement with a similar donor strength of CH_2Cl_2 and BF_4^- , the triflate complexes **8a–d** are undissociated in CH_2Cl_2 due to the markedly higher strength of OTf[−]. In THF solution all these complexes generate the ionic THF-solvates **9a–d(Y)**, with the distinction that for triflate as the anion undissociated **8a–d** and ionic **9a–d(OTf)** appear in a balanced equilibrium, suggesting that OTf[−] and THF have a similar donor strength. In all complexes mentioned so far the solvate ligands (CH_2Cl_2 , THF) or anions (BF_4^- , OTf[−]) are displaced by water to give **10a–d(Y)**. In the end, the chlorides **6a–d** show a solvent effect with THF-*d*₈ (but not any more with CD_2Cl_2) in the NMR spectra, suggesting weak and reversible THF solvation, whereas the limiting PdMe complexes **7a–d**, obtained from **6a–d** with LiMe by substituting Cl[−] for methyl, appear independent of both solvents.

Because of the low, yet real donor strength of CH_2Cl_2 and similar solvents, it seems likely that equally or weaker coordinating anions than $Y = \text{PF}_6$ and AlR_4^+ (e.g., $\text{B}(\text{C}_6\text{F}_5)_4^-$, $\text{B}\{\text{C}_6\text{H}_3\text{-}3,5\text{-(CF}_3)_2\}_4^-$, or carborates) will also give solvate complexes of the type **11a,c(Y)**, differing merely in the counterion. Thus, for very weakly coordinating anions the accessibility of solvent-free complexes $[(\pi\text{-allyl})\text{Pd}(\text{NHC})]^+\text{Y}^-$ from a solution is limited by the solvent donor strength. However, crystalline $[(\pi\text{-allyl})\text{Pd}(\text{NHC})]^+\text{Y}^-$ may possibly be attainable by subjecting ionic $[(\pi\text{-allyl})\text{Pd}(\text{NHC})(\text{L})]^+\text{Y}^-$ crystals containing weakly coordinating and simultaneously quite volatile ligands such as CH_2Cl_2 , SO_2 , or C_2H_4 to vacuum with loss of L and retention of the lattice. A similar approach served for the synthesis of **13a,c** and **14a,c**, although these products proved unsuited for X-ray structure determination.

Conclusions

We have described the synthesis and properties of the so far elusive cationic solvent complexes $[(\pi\text{-allyl})\text{Pd}(\text{NHC})(\text{S})]\text{Y}$ with $\text{S} = \text{THF}$ (**9**) and CH_2Cl_2 (**11**). The presence of a dinuclear complex with a bridging CH_2Cl_2 ligand, $[(\pi\text{-C}_3\text{H}_5)\text{Pd}(\text{NHC})]_2\text{-}(\mu\text{-CH}_2\text{Cl}_2)]\text{PF}_6$ (**13**), seems also possible. In addition, the neutral adducts $(\pi\text{-allyl})\text{Pd}(\text{NHC})\text{Y}$ with weakly coordinating anions $Y = \text{OTf}$ (**8**), BF_4 (**12**), and AlR_4^+ (**14**) have been obtained either by halide abstraction of the chlorides **6** with AgY (**8** and **12**) or by evaporation of weakly coordinated solvent ligands (**14**). For BF_4 , the most nucleophilic of the given series of complex anions, the solvent-free BF_4 adduct **12c** separates directly from CH_2Cl_2 solution.

For complexes having the *N*-aryl-substituted NHC ligand the synthesis of products with OTf (**8c,d**) and BF_4 groups (**9c(BF₄)** and **12c**) is also possible by protolysis of the PdMe complexes **7c,d** with HOTf or HBF_4 . In contrast, when starting from **7a,b** the *N*-^tBu-substituted NHC ligand becomes protonated even by weak acids to give the corresponding imidazolium salt, resulting in degradation of the products.

The chloride abstraction from **6** with AgY ($Y = \text{BF}_4, \text{PF}_6, \text{AlR}_4^+$) most likely proceeds via the formation of an intermediate cationic $\text{Pd}_2(\mu\text{-Cl})$ complex of type **4**. From these the bridging chloride can be abstracted by AgY reagents, whereas abstraction with TiY fails.

Most of the complexes in this investigation are thermally stable and crystalline, and, in addition to the THF-solvate **9a(BF₄)**, both the ionic CH_2Cl_2 -solvate **11c(PF₆)** and the neutral

BF_4 adduct **12a** have been characterized by X-ray structure analyses. Moreover, the novel “donor-free” $(\pi\text{-allyl})\text{Pd}$ -triflates **5a,b**, of which the parent **5a** was shown to have a helical chain structure in the solid, turn out to be useful reagents.

Experimental Part

All manipulations were carried out under argon with Schlenk-type glassware. Solvents were dried prior to use by distillation from NaAlEt_4 . $\{(\eta^3\text{-C}_3\text{H}_5)\text{PdCl}\}_2$,⁴³ $\{(\eta^3\text{-MeC}_3\text{H}_4)\text{PdCl}\}_2$,⁴⁴ NHCs,⁴⁵ (tmeda) MgMe_2 ,^{22b} **6a**,^{14b,21b} **6c**,^{14b,21} and $[\text{Ag}(\text{CH}_2\text{Cl}_2)]\text{Al}\{\text{OC}(\text{CF}_3)_3\}_4$ ^{31a} were prepared as published. The slightly impure AgPF_6 was obtained from Aldrich. It was purified by recrystallization from diethyl ether. Addition of benzene to the ethereal solution and cooling to -25°C afforded colorless crystalline $[\text{Ag}(\text{C}_6\text{H}_6)_2]\text{PF}_6$.⁴⁶ Microanalyses were performed by the local Mikroanalytisches Labor Kolbe. EI mass spectra were recorded at 70 eV and refer to ¹¹B, ³⁵Cl, and ¹⁰⁶Pd. For the ESI mass spectra an ESQ3000 instrument was used. ¹H NMR spectra were measured at 300 MHz and ¹³C NMR spectra at 75.5 MHz (both relative to TMS) on Bruker AMX-300 and DPX-300 instruments. The given NMR data refer to solutions of the compounds in CD_2Cl_2 . DSC spectra were recorded with the Mettler-Toledo TA8000 thermal analysis system having a DSC820 measuring module.

$\{(\eta^3\text{-C}_3\text{H}_5)\text{Pd}(\mu\text{-OTf})\}_n$ (**5a**). A mixture of $\{(\eta^3\text{-C}_3\text{H}_5)\text{Pd}(\mu\text{-Cl})\}_2$ (183 mg, 0.50 mmol) and AgOTf (257 mg, 1.00 mmol) in 20 mL of Et_2O was stirred at room temperature for 30 min. The precipitated AgCl was removed by filtration. Keeping the solution at -40°C for 2 days afforded yellow crystals: yield 240 mg (81%). EI-MS (135 °C): *m/e* (%) 592 ($[\text{2M}]^+$, 16), 443 ($[\text{2M} - \text{OTf}]^+$, 8), 402 ($[(\text{C}_3\text{H}_5)\text{Pd}_2(\text{OTf})]^+$, 14), 296 ($[\text{M}]^+$, 14), 147 ($[(\text{C}_3\text{H}_5)\text{Pd}]^+$, 100). ESIpos-MS (THF): *m/e* (%) 443 ($[\text{2M} - \text{OTf}]^+$, 10), 147 ($[(\text{C}_3\text{H}_5)\text{-Pd}]^+$, 100). Anal. Calcd for $\text{C}_4\text{H}_5\text{F}_3\text{O}_3\text{PdS}$ (296.6): C, 16.20; H, 1.70; F, 19.22; O, 16.19; Pd, 35.89; S, 10.81. Found: C, 16.10; H, 1.77; F, 19.36; Pd, 35.82; S, 10.72.

$\{(\eta^3\text{-2-MeC}_3\text{H}_4)\text{Pd}(\mu\text{-OTf})\}_2$ (**5b**). $\{(\eta^3\text{-2-MeC}_3\text{H}_4)\text{Pd}(\mu\text{-Cl})\}_2$ (197 mg, 0.50 mmol) was treated with AgOTf (257 mg, 1.00 mmol) in 15 mL of CH_2Cl_2 for 30 min (20°C). Workup was as for **5a**. Cooling the solution to -60°C afforded fine yellow needles: yield 185 mg (59%). EI-MS (115 °C): *m/e* (%) 620 ($[\text{M}]^+$, 12), 471 ($[\text{M} - \text{OTf}]^+$, 9), 416 ($[\text{M} - \text{OTf} - \text{C}_3\text{H}_4\text{Me}]^+$, 7), 310 ($[\text{M}/2]^+$, 10), 161 ($[(\text{C}_3\text{H}_4\text{Me})\text{Pd}]^+$, 60). Anal. Calcd for $\text{C}_{10}\text{H}_{14}\text{F}_6\text{O}_6\text{Pd}_2\text{S}_2$ (621.2): C, 19.34; H, 2.27; F, 18.35; O, 15.45; Pd, 34.26; S, 10.32. Found: C, 19.18; H, 2.06; Pd, 34.11; S, 10.30.

$(\eta^3\text{-MeC}_3\text{H}_4)\text{Pd}\{\text{C}(\text{N}(\text{tBu})\text{CH}_2)\}_2\text{Cl}$ (**6b**).^{20a} Solutions of $\{(\eta^3\text{-MeC}_3\text{H}_4)\text{PdCl}\}_2$ (394 mg, 1.00 mmol) in 5 mL of CH_2Cl_2 and $\text{C}(\text{N}(\text{tBu})\text{CH}_2)$ (361 mg, 2.00 mmol) in 15 mL of diethyl ether were combined at 0°C . After 1 h the mixture was cooled to -78°C to afford off-white microcrystals: yield 380 mg (50%). EI-MS (120 °C): *m/e* (%) 376 ($[\text{M}]^+$, 18), 286 ($[(\text{NHC})\text{Pd}]^+$, 100), 229 ($[(\text{NHC})\text{Pd} - \text{tBu}]^+$, 56). $\text{C}_{15}\text{H}_{27}\text{ClN}_2\text{Pd}$ (377.3).

$(\eta^3\text{-MeC}_3\text{H}_4)\text{Pd}\{\text{C}(\text{N}(\text{C}_6\text{H}_3\text{-}2,6\text{-iPr}_2)\text{CH}_2)\}_2\text{Cl}$ (**6d**).^{20b} A mixture of $\{(\eta^3\text{-MeC}_3\text{H}_4)\text{PdCl}\}_2$ (394 mg, 1.00 mmol) and $\text{C}(\text{N}(\text{C}_6\text{H}_3\text{-}2,6\text{-iPr}_2)\text{CH}_2)$ (777 mg, 2.00 mmol) in 20 mL of CH_2Cl_2 was stirred at 20°C for 1 h. The solution was concentrated in a vacuum to about 10 mL, and an equal volume of diethyl ether was added. Cooling to -78°C gave colorless microcrystals, which were filtered off,

(43) (a) Dent, W. T.; Long, R.; Wilkinson, A. J. *J. Chem. Soc.* **1964**, 1585. (b) Tatsuno, Y.; Yoshida, T.; Otsuka, S. *Inorg. Synth.* **1979**, *19*, 220.

(44) Krause, J.; Bonrath, W.; Pörschke, K.-R. *Organometallics* **1992**, *11*, 1158, and references therein.

(45) (a) Arduengo, A. J., III; Bock, H.; Chen, H.; Denk, M.; Dixon, D. A.; Green, J. C.; Herrmann, W. A.; Jones, N. L.; Wagner, M.; West, R. *J. Am. Chem. Soc.* **1994**, *116*, 6641. (b) Jafarpour, L.; Stevens, E. D.; Nolan, S. P. *J. Organomet. Chem.* **2000**, *606*, 49. (c) Arduengo, A. J., III; Krafczyk, R.; Schmutzler, R.; Craig, H. A.; Goerlich, J. R.; Marshall, W. J.; Unverzagt, M. *Tetrahedron* **1999**, *55*, 14523.

(46) Sharp, D. W. A.; Sharpe, A. G. *J. Chem. Soc.* **1956**, 1855.

washed with cold ether, and dried under vacuum: yield 490 mg (42%). EI-MS (135 °C): *m/e* (%) 584 ([M]⁺, 1), 494 ([Pd(NHC)]⁺, 29), 387 ([NHC - H]⁺, 100). ESIPos-MS (THF): *m/e* (%) 549 ([M - Cl]⁺, 80), 389 ([NHC + H]⁺, 100). C₃₁H₄₃ClN₂O₃Pd (585.6).

(η^3 -C₃H₅)Pd{C(N('Bu)CH₂)₂Me} (7a). A solution of **6a** (363 mg, 1.00 mmol) and (tmeda)MgMe₂ (85 mg, 0.50 mmol) in 15 mL of diethyl ether was stirred at ambient temperature for 3 h. After removal of the volatiles under vacuum the residue was extracted twice with 10 mL of pentane and the solution was concentrated to about 10 mL. Cooling to -40 °C for 2 days afforded colorless crystals: yield 223 mg (65%). EI-MS (55 °C): *m/e* (%) 342 ([M]⁺, 2), 327 ([M - Me]⁺, 51), 285 ([NHC]Pd - H]⁺, 100), 229 ([NHC]Pd - 'Bu]⁺, 64), 181 ([NHC + H]⁺, 34). ESIPos-MS (THF): *m/e* (%) 327 ([M - Me]⁺, 55), 301 ([M - ally]⁺, 40), 195 ([MeC(N('Bu)CH₂)₂]⁺, 100). For NMR data, see Table 2. Anal. Calcd for C₁₅H₂₈N₂Pd (342.8): C, 52.55; H, 8.23; N, 8.17; Pd, 31.04. Found: C, 52.42; H, 8.36; N, 8.10; Pd, 30.89.

(η^3 -MeC₃H₄)Pd{C(N('Bu)CH₂)₂Me} (7b). Synthesis was as for **7a**, but starting from **6b** (377 mg, 1.00 mmol). Colorless crystals: yield 235 mg (66%). EI-MS (50 °C): *m/e* (%) 356 ([M]⁺, 1), 341 ([M - Me]⁺, 45), 285 ([NHC]Pd - H]⁺, 100), 229 ([NHC]Pd - 'Bu]⁺, 63). ESIPos-MS (THF): *m/e* (%) 341 ([M - Me]⁺, 20), 301 ([M - ally]⁺, 50), 195 ([MeC(N('Bu)CH₂)₂]⁺, 100). For NMR data, see Table S2. C₁₆H₃₀N₂Pd (356.9).

(η^3 -C₃H₅)Pd{C(N(C₆H₃-2,6-ⁱPr₂)CH₂)₂Me} (7c). Synthesis was as described in ref 14b to give light yellow rods. ESIPos-MS (THF): *m/e* (%) 535 ([M - Me]⁺, 100). For NMR data, see Table 3. C₃₁H₄₄N₂Pd (555.1).

(η^3 -MeC₃H₄)Pd{C(N(C₆H₃-2,6-ⁱPr₂)CH₂)₂Me} (7d). To a solution of **6d** (586 mg, 1.00 mmol) in 15 mL of diethyl ether was added a 1.7 M ethereal solution of LiMe (0.65 mL, 1.1 mmol) at -40 °C. The mixture was allowed to warm to ambient temperature and was stirred for 3 h. After removal of the volatiles under vacuum the residue was extracted twice with 10 mL of pentane. Cooling to -40 °C afforded colorless crystals: yield 225 mg (40%). EI-MS (110 °C): *m/e* (%) 564 ([M]⁺, 1), 549 ([M - Me]⁺, 38), 494 ([Pd(NHC)]⁺, 3), 387 ([NHC - H]⁺, 100). ESIPos-MS (THF): *m/e* (%) 549 ([M - Me]⁺, 100). For NMR data, see Table S3. C₃₂H₄₆N₂Pd (565.2).

(η^3 -C₃H₅)Pd{C(N('Bu)CH₂)₂OTf} (8a). **Route a**. The solutions of **5a** (297 mg, 1.00 mmol Pd) and C(N('Bu)CH₂)₂ (180 mg, 1.00 mmol), each in 20 mL of diethyl ether, were combined at 20 °C. After a few minutes pale yellow crystals separated. For complete crystallization the flask was slowly cooled to -20 °C: yield 335 mg (70%). **Route b**. A mixture of **6a** (363 mg, 1.00 mmol) and AgOTf (257 mg, 1.00 mmol) in 20 mL of Et₂O was stirred at room temperature for 2 h. The precipitated AgCl was removed by filtration. Cooling the solution to -40 °C and further to -78 °C afforded pale yellow microcrystals: yield 320 mg (67%). EI-MS (135 °C): *m/e* (%) 476 ([M]⁺, 3), 327 ([M - OTf]⁺, 7), 285 ([Pd(NHC) - H]⁺, 100). ESIPos-MS (THF): *m/e* (%) 327 ([M - OTf]⁺, 100). For NMR data, see Table 2. Anal. Calcd for C₁₅H₂₅F₃N₂O₃Pd (476.9): C, 37.78; H, 5.28; F, 11.95; N, 5.87; O, 10.07; Pd, 22.32; S, 6.72. Found: C, 37.57; H, 5.28; N, 5.79; Pd, 22.18; S, 6.67.

(η^3 -MeC₃H₄)Pd{C(N('Bu)CH₂)₂OTf} (8b). Synthesis was as for **8a**, route b, but starting from **6b** (377 mg, 1.00 mmol). Pale yellow microcrystals: yield 335 mg (68%). EI-MS (135 °C): *m/e* (%) 490 ([M]⁺, 7), 341 ([M - OTf]⁺, 6), 285 ([Pd(NHC) - H]⁺, 100). ESIPos-MS (THF): *m/e* (%) 341 ([M - OTf]⁺, 100). For NMR data, see Table S2. C₁₆H₂₇F₃N₂O₃Pd (490.9).

(η^3 -C₃H₅)Pd{C(N(C₆H₃-2,6-ⁱPr₂)CH₂)₂OTf} (8c). A mixture of **6c** (286 mg, 0.50 mmol) and AgOTf (131 mg, 0.51 mmol) in 20 mL of Et₂O was stirred at 20 °C for 1 h. The precipitated AgCl was removed by filtration. Keeping the solution at -40 °C for 2 days afforded colorless microcrystals: yield 230 mg (67%). EI-MS (210 °C): *m/e* (%) 684 ([M]⁺, 1), 535 ([M - OTf]⁺, 1), 494

([Pd(NHC)]⁺, 48), 387 ([NHC - H]⁺, 100). ESIPos-MS (CH₂-Cl₂): *m/e* (%) 535 ([M - OTf]⁺, 100). For NMR data, see Table 3. C₃₁H₄₁F₃N₂O₃PdS (685.2).

(η^3 -MeC₃H₄)Pd{C(N(C₆H₃-2,6-ⁱPr₂)CH₂)₂OTf} (8d). **Route a**. A solution of **5b** (194 mg, 0.50 mmol of Pd) in 10 mL of diethyl ether was added to a suspension of C(N(C₆H₃-2,6-ⁱPr₂)CH₂) (155 mg, 0.50 mmol) in 5 mL of diethyl ether (20 °C). The mixture was stirred for a few minutes so that a clear solution was obtained. Cooling the solution to -40 °C afforded colorless microcrystals, which were isolated and dried under vacuum: yield 300 mg (86%). **Route b**. Synthesis was as for **8c** but starting from **6d** (293 mg, 0.50 mmol). Colorless microcrystals: yield 238 mg (68%). **Route c**. To a solution of **7d** (283 mg, 0.50 mmol) in 15 mL of diethyl ether was added HOTf (0.044 mL, 0.50 mmol) at -40 °C. Keeping the solution at -40 °C for 2 days afforded colorless microcrystals: yield 332 mg (95%). EI-MS (176 °C): *m/e* (%) 698 ([M]⁺, 3), 549 ([M - OTf]⁺, 3), 494 ([Pd(NHC)]⁺, 43), 387 ([NHC - H]⁺, 100). ESIPos-MS (THF): *m/e* (%) 549 ([M - OTf]⁺, 100). For NMR data, see Table S3. Anal. Calcd for C₃₂H₄₃F₃N₂O₃PdS (699.2): C, 54.97; H, 6.20; Pd, 15.22; S, 4.59. Found: C, 54.98; H, 6.30; Pd, 15.73; S, 4.32.

(η^3 -C₃H₅)Pd{C(N('Bu)CH₂)₂}(THF)]BF₄ (9a(BF₄)). A mixture of **6a** (363 mg, 1.00 mmol) and AgBF₄ (195 mg, 1.00 mmol) in 30 mL of THF was stirred at 20 °C for 1 h. After removal of AgCl by filtration the yellow solution was cooled to -40 °C. In the course of several days pale yellow crystals precipitated, which were isolated and dried at 20 °C under vacuum: yield 265 mg (54%). ESIPos-MS (CH₂Cl₂): *m/e* (%) 327 ([M - THF - BF₄]⁺, 100). ESIneg-MS (CH₂Cl₂): *m/e* (%) 87 ([BF₄]⁻, 100). For NMR data, see Table 2. Anal. Calcd for C₁₈H₃₃BF₄N₂OPd (486.7): C, 44.42; H, 6.83; B, 2.22; F, 15.61; N, 5.76; O, 3.29; Pd, 21.87. Found: C, 44.12; H, 6.65; B, 2.17; F, 14.79; Pd, 20.55.

(η^3 -C₃H₅)Pd{C(N('Bu)CH₂)₂}(THF)]PF₆ (9a(PF₆)). A mixture of **6a** (363 mg, 1.00 mmol) and [Ag(C₆H₆)₂]PF₆ (409 mg, 1.00 mmol) in 15 mL of THF was stirred at -20 °C for 1 h. After removal of the precipitated AgCl by filtration the light yellow solution was concentrated under vacuum to a volume of 10 mL. About 2 mL of Et₂O was added dropwise. Cooling the solution to 0 °C and then to -25 °C afforded pale yellow microcrystals: yield 255 mg (47%). ESIPos-MS (CH₂Cl₂): *m/e* (%) 327 ([M - THF - PF₆]⁺, 100), 285 ([NHC]Pd - H]⁺, 45). ESIneg-MS (CH₂Cl₂): *m/e* (%) 145 ([PF₆]⁻, 100). For NMR data, see Table 2. C₁₈H₃₃F₆N₂-OPd (544.9).

(η^3 -C₃H₅)Pd{C(N('Bu)CH₂)₂}(THF)]Al{OC(CF₃)₃}₄ (9a(Al-R^F₄)). The complex **11a(AlR^F₄)** (690 mg, 0.50 mmol) was dissolved in 1 mL of THF, and 1 mL of CH₂Cl₂ was added (20 °C). Cooling the pale yellow solution to -40 °C for 3 days afforded light yellow crystals: yield 506 mg (74%). For NMR data, see Table 2. Anal. Calcd for C₁₈H₃₃N₂OPd·AlC₁₆F₃₆O₄ (1367.0): C, 29.87; H, 2.43; Al, 1.97; F, 50.03; N, 2.05; O, 5.85; Pd, 7.78. Found: C, 30.14; H, 2.45; Al, 1.94; F, 50.18; Pd, 7.67.

(η^3 -C₃H₅)Pd{C(N(C₆H₃-2,6-ⁱPr₂)CH₂)₂}(THF)]BF₄ (9c(BF₄)). To the solution of **6c** (572 mg, 1.00 mmol) in 20 mL of THF was added AgBF₄ (195 mg, 1.00 mmol). The mixture was stirred at 20 °C for 1 h, and the precipitated AgCl was removed by filtration. Keeping the solution at -40 °C for 1 day afforded off-white crystals, which were isolated and dried under vacuum at -30 °C: yield 495 mg (71%). ESIPos-MS (CH₂Cl₂): *m/e* (%) 535 ([M - THF - BF₄]⁺, 100). ESIneg-MS (CH₂Cl₂): *m/e* (%) 87 ([BF₄]⁻, 100). For NMR data, see Table 3. C₃₄H₄₉BF₄N₂OPd (695.0).

(η^3 -C₃H₅)Pd{C(N(C₆H₃-2,6-ⁱPr₂)CH₂)₂}(THF)]PF₆ (9c(PF₆)). A mixture of **6c** (571 mg, 1.00 mmol) and [Ag(C₆H₆)₂]PF₆ (409 mg, 1.00 mmol) in 20 mL of THF was stirred at -20 °C for 1 h. The precipitated AgCl was removed by filtration. After addition of about 5 mL of Et₂O the solution was cooled to 0 °C and then -25 °C to afford off-white crystals: yield 360 mg (48%). ESIPos-MS (CH₂Cl₂): *m/e* (%) 535 ([M - THF - PF₆]⁺, 100). ESIneg-

MS (CH₂Cl₂): *m/e* (%) 145 ([PF₆][−], 100). For NMR data, see Table 3. C₃₄H₄₉F₆N₂OPd (753.2).

[(η^3 -C₃H₅)Pd{C(N(C₆H₃-2,6-*i*-Pr₂)CH)₂}(THF)]Al{OC(CF₃)₃}₄ (**9c**(AIR^F₄)). A solution of **6c** (571 mg, 1.00 mmol) and [Ag(CH₂Cl₂)]Al{OC(CF₃)₃}₄ (1160 mg, 1.00 mmol) in 30 mL of CH₂Cl₂ was stirred for 30 min (20 °C). After removal of the precipitated AgCl by filtration the solution was concentrated under vacuum to a volume of 15 mL, and 1 mL of THF was added. Cooling the solution from −40 to −78 °C afforded off-white crystals: yield 1.19 g (76%). ESIPos-MS (CH₂Cl₂): *m/e* (%) 535 ([M – THF – AIR^F₄]⁺, 100). ESIneg-MS (CH₂Cl₂): *m/e* (%) 967 ([Al{OC(CF₃)₃}₄][−], 100). For NMR data, see Table 3. Anal. Calcd for C₃₄H₄₉N₂OPd·AlC₁₆F₃₆O₄ (1575.3): C, 38.12; H, 3.14; Al, 1.71; F, 43.42; N, 1.78; O, 5.08; Pd, 6.76. Found: C, 40.67; H, 3.19; Al, 1.67; F, 42.05; Pd, 6.74.

[(η^3 -C₃H₅)Pd{C(N(**Bu**)CH)₂}(CH₂Cl₂)]Al{OC(CF₃)₃}₄ (**11a**(AIR^F₄)). A solution of **6a** (363 mg, 1.00 mmol) and [Ag(CH₂Cl₂)]Al{OC(CF₃)₃}₄ (1160 mg, 1.00 mmol) in 30 mL of CH₂Cl₂ was stirred for 30 min (20 °C). After filtration from the precipitated AgCl the solution was slowly cooled to −78 °C to afford intense yellow microcrystals, which were dried at −40 °C under vacuum: yield 745 mg (54%). ESIPos-MS (CH₂Cl₂): *m/e* (%) 327 ([M – CH₂Cl₂ – AIR^F₄]⁺, 100). ESIneg-MS (CH₂Cl₂): *m/e* (%) 967 ([Al{OC(CF₃)₃}₄][−], 100). For NMR data, see Table 2. Anal. Calcd for C₁₅H₂₇Cl₂N₂Pd·AlC₁₆F₃₆O₄ (1379.8): C, 26.98; H, 1.97; Al, 1.96; F, 49.57; Pd, 7.71. Found: C, 27.43; H, 1.91; Al, 1.94; F, 49.58; Pd, 7.85.

[(η^3 -C₃H₅)Pd{C(N(C₆H₃-2,6-*i*-Pr₂)CH)₂}(CH₂Cl₂)]PF₆·2CH₂Cl₂ (**11c**(PF₆)). A mixture of **6c** (572 mg, 1.00 mmol) and AgPF₆ (253 mg, 1.00 mmol) in 20 mL of CH₂Cl₂ was stirred at 20 °C for 1 h. The precipitated AgCl was removed by filtration, and pentane (5 mL) was added. Cooling to −25 °C for 4 days afforded pale yellow crystals, which were dried under vacuum at −30 °C: yield 700 mg (75%). ESIPos-MS (CH₂Cl₂): *m/e* (%) 535 ([M – 3 CH₂Cl₂ – PF₆]⁺, 100). For NMR data, see Table 3. C₃₃H₄₇Cl₆F₆N₂PPd (935.9). Correct elemental analysis of the compound appeared difficult, presumably due to ready hydrolysis of PF₆ and loss of CH₂Cl₂.

[(η^3 -C₃H₅)Pd{C(N(C₆H₃-2,6-*i*-Pr₂)CH)₂}(CH₂Cl₂)]Al{OC(CF₃)₃}₄ (**11c**(AIR^F₄)). A solution of **6c** (572 mg, 1.00 mmol) and [Ag(CH₂Cl₂)]Al{OC(CF₃)₃}₄ (1160 mg, 1.00 mmol) in 30 mL of CH₂Cl₂ was stirred for 30 min (20 °C). After filtration from the precipitated AgCl the solution was concentrated under vacuum to a volume of 15 mL, and a few drops of pentane were added. Cooling of the solution from −40 to −78 °C afforded large clusters of yellow microcrystals, which were isolated and dried under vacuum at −40 °C: yield 1.48 g (93%). ESIPos-MS (CH₂Cl₂): *m/e* (%) 535 ([M – CH₂Cl₂ – AIR^F₄]⁺, 100). ESIneg-MS (CH₂Cl₂): *m/e* (%) 967 ([Al{OC(CF₃)₃}₄][−], 100). For NMR data, see Table 3. Anal. Calcd for C₃₁H₄₃Cl₂N₂Pd·AlC₁₆F₃₆O₄ (1588.1): C, 35.55; H, 2.73; Al, 1.70; Cl, 4.46; F, 43.07; N, 1.76; O, 4.03; Pd, 6.70. Found: C, 35.94; H, 2.79; Al, 1.70; F, 42.80; Pd, 6.70.

(η^3 -C₃H₅)Pd{C(N(**Bu**)CH)₂}(BF₄) (**12a**). A mixture of **6a** (363 mg, 1.00 mmol) and AgBF₄ (195 mg, 1.00 mmol) in 30 mL of toluene was stirred at ambient temperature for 2 h. The precipitated AgCl was removed by filtration. Slow crystallization between −25 and −80 °C afforded yellow crystals: yield 250 mg (60%). ESIPos-MS (CH₂Cl₂): *m/e* (%) 327 ([M – BF₄]⁺, 100). For NMR data, see Table 2. Anal. Calcd for C₁₄H₂₅BF₄N₂Pd (414.6): C, 40.56; H, 6.08; B, 2.61; F, 18.33; N, 6.76; Pd, 25.67. Found: C, 40.36; H, 6.12; B, 2.64; F, 18.38; Pd, 25.66.

(η^3 -C₃H₅)Pd{C(N(C₆H₃-2,6-*i*-Pr₂)CH)₂}(BF₄) (**12c**). **Route a.** A solution of **6c** (286 mg 0.50 mmol) and AgBF₄ (98 mg, 0.50 mmol) in 20 mL of CH₂Cl₂ was stirred for 1 h (20 °C). The precipitated AgCl was removed by filtration. The solution was concentrated under vacuum to 10 mL, and an equal volume of pentane was added. Slow cooling from −25 to −80 °C gave pale yellow crystals, which were isolated and dried under vacuum (20 °C): yield 130 mg (42%). **Route b.** To a solution of **7c** (139 mg, 0.25 mmol) in 10 mL of CH₂Cl₂ was added a 54% HBF₄ solution in Et₂O (0.035 mL, 0.254 mmol) at −30 °C. Cooling the solution to −40 °C for 1 day yielded pale yellow needles: yield 115 mg (74%). ESIPos-MS (CH₂Cl₂): *m/e* (%) 535 ([M – BF₄]⁺, 100). For NMR data, see Table 3. Anal. Calcd for C₃₀H₄₁BF₄N₂Pd (622.9): C, 57.85; H, 6.63; B, 1.74; F, 12.20; N, 4.50; Pd, 17.08. Found: B, 1.82; F, 12.04; Pd, 16.93.

(η^3 -C₃H₅)Pd{C(N(**Bu**)CH)₂}(PF₆)·1/2CH₂Cl₂ (**13a**). A solution of **6a** (363 mg, 1.00 mmol) in 10 mL of CH₂Cl₂ was stirred with [Ag(C₆H₆)₂]PF₆ (409 mg, 1.00 mmol) at −20 °C for 30 min. After removal of the precipitated AgCl by filtration the solution was concentrated under vacuum to a volume of 5 mL, and 2 mL of pentane was added. The solution was slowly cooled from 0 to −40 °C to afford yellow microcrystals, which were dried under vacuum at −20 °C: yield 275 mg (53%). An almost quantitative yield is obtained by evaporating the solvent to dryness. The compound retained about 1/2 CH₂Cl₂ when kept in a vacuum at ambient temperature for 2 h. For NMR data, see Table 2. ESIPos-MS (CH₂Cl₂): *m/e* (%) 327 ([M – PF₆]⁺, 100). Anal. Calcd for C₁₄H₂₅F₆N₂PPd·1/2CH₂Cl₂ (515.2): C, 33.80; H, 5.09; Cl, 6.88; F, 22.12; N, 5.44; P, 6.01; Pd, 20.66. Found: C, 33.04; H, 5.28; P, 6.53; Pd, 19.20.

(η^3 -C₃H₅)Pd{C(N(C₆H₃-2,6-*i*-Pr₂)CH)₂}(PF₆)·1/2CH₂Cl₂ (**13c**). The synthesis was performed as for **11c**(PF₆), but the isolated pale yellow crystals were dried under vacuum at 20 °C for 1 h: yield 510 mg (70%). ESIPos-MS (CH₂Cl₂): *m/e* (%) 535 ([M – PF₆]⁺, 100). The compound retained about 1/2 CH₂Cl₂ when kept in a vacuum at ambient temperature for 2 h. For NMR data, see Table 3. Anal. Calcd for C₃₀H₄₁F₆N₂PPd·[1/2]CH₂Cl₂ (723.5): C, 50.63; H, 5.85; Cl, 4.90; F, 15.75; N, 3.87; P, 4.28; Pd, 14.71. Found: C, 49.45; H, 5.61; F, 15.69; P, 4.19; Pd, 14.85.

(η^3 -C₃H₅)Pd{C(N(**Bu**)CH)₂}(Al{OC(CF₃)₃})₄ (**14a**). Complex **11a**(AIR^F₄) (690 mg, 0.50 mmol) was kept under vacuum at ambient temperature for 2 h to afford a yellow powder: yield 650 mg (100%). ESIPos-MS (CH₂Cl₂): *m/e* (%) 327 ([M – AIR^F₄]⁺, 100). ESIneg-MS (CH₂Cl₂): *m/e* (%) 967 ([Al{OC(CF₃)₃})₄][−], 100). For NMR data, see Table 2. Anal. Calcd for C₁₄H₂₅N₂Pd·AlC₁₆F₃₆O₄ (1294.9): C, 27.83; H, 1.95; Al, 2.08; F, 52.82; N, 2.16; O, 4.94; Pd, 8.22. Found: C, 27.85; H, 2.01; Al, 2.03; F, 52.69; Pd, 8.20.

(η^3 -C₃H₅)Pd{C(N(C₆H₃-2,6-*i*-Pr₂)CH)₂}(Al{OC(CF₃)₃})₄ (**14c**). The isolated crystals of **11c**(AIR^F₄) (794 mg, 0.50 mmol) were kept under vacuum at ambient temperature for 2 h to afford a pale yellow powder: yield 750 mg (100%). ESIPos-MS (CH₂Cl₂): *m/e* (%) 535 ([M – AIR^F₄]⁺, 100). ESIneg-MS (CH₂Cl₂): *m/e* (%) 967 ([Al{OC(CF₃)₃})₄][−], 100). For NMR data, see Table 3. Anal. Calcd for C₃₀H₄₁N₂Pd·AlC₁₆F₃₆O₄ (1503.2): C, 36.76; H, 2.75; Al, 1.79; F, 45.50; N, 1.86; O, 4.26; Pd, 7.08. Found: C, 36.70; H, 3.10; Al, 1.79; F, 45.22; Pd, 6.96.

Supporting Information Available: Tables S1–S3, Figures S2 and S3, and CIF data for **5a**, **9a**(BF₄), **11c**(PF₆), and **12a**. This material is available free of charge via the Internet at <http://pubs.acs.org>.

OM0702274